Detrital zircon U-Pb-Hf isotopes and whole-rock geochemistry of Ediacaran - Silurian clastic sediments of the Uzbek Tienshan: sources and tectonic implications

Dmitry Konopelko, Inna Safonova, Alina Perfilova, Yury Biske, Rustam Mirkamalov, Farid Divaev, Pavel Kotler, Olga Obut, Bo Wang, Min Sun & Natalia Soloshenko

Taylor & Francis
Taylor & Francis Group

Check for updates

Detrital zircon U-Pb-Hf isotopes and whole-rock geochemistry of Ediacaran - Silurian clastic sediments of the Uzbek Tienshan: sources and tectonic implications

Dmitry Konopelko[a,b], Inna Safonova[b,c], Alina Perfilova[b,c], Yury Biske[a], Rustam Mirkamalov[d], Farid Divaev[d], Pavel Kotler[b,c], Olga Obut[e], Bo Wang[f], Min Sun[g] and Natalia Soloshenko[h]

[a]Institute of Earth Sciences, St. Petersburg State University, St. Petersburg Russia; [b]Geology-Geophysics Department, Novosibirsk State University Novosibirsk, Russia; [c]Sobolev Institute of Geology and Mineralogy SB RAS, Novosibirsk, Russia; [d]Institute of Mineral Resources, Tashkent, Uzbekistan; [e]Trofimuk Institute of Petroleum Geology and Geophysics SB RAS Novosibirsk, Russia; [f]State Key Laboratory for Mineral Deposits Research, Department of Earth Sciences, Nanjing University, Nanjing, China; [g]Department of Earth Sciences, The University of Hong Kong, Hong Kong, China; [h]Zavaritskiy Institute of Geology and Geochemistry UrB RAS, Yekaterinburg, Russia

ABSTRACT

The paper presents first high-precision data, U-Pb detrital zircon ages, whole-rock geochemistry, Hf-in-zircon and whole-rock Nd isotopes, from pre-Devonian (Ediacaran and Silurian) clastic sediments (sandstones) of the Tamdytau, Bukantau and Nuratau mountainous ranges of the Kyzylkum Desert and Nuratau Range in the western Uzbek Tienshan. The sediments form a turbidite-type complex associated with ocean plate stratigraphy units (oceanic pillow basalt, chert, siliceous mudstone and siltstone) and arc volcanic rocks. Four sandstone samples from the Tamdytau and Northern Nuratau Mts. (Besapan and Kaltadavan formations, respectively) yielded maximum depositional ages in the range of 570–540 Ma. These ages indicate the formation of pre-Devonian sedimentary units during a relatively narrow time interval from the latest Neoproterozoic (Ediacaran) to the earliest Cambrian, i.e. ca. 50–70 Myr. Five samples of turbidites from the Bukantau Mts. (Baimen Fm.) yielded a maximal depositional age of ca. 440 Ma, i.e. early Silurian (Llandovery). The petrographic, major and trace element compositions, as well as εNd(t) values ranging from -16 to -9 of those sandstones suggest their generally mature character and derivation from recycled orogens with a limited contribution of juvenile crust material. All sandstone samples yielded similar detrital zircon U-Pb age patterns characterized by major peaks at 650–570, 870–730, 1050–900 and 2400 Ma and by a smaller peak at ca. 1800 Ma. These patterns are similar to the U-Pb age spectra from the basement of the Tarim Craton. However, the Kyzylkum basement may contain a larger proportion of late Archaean rocks and igneous formations related to Ediacaran – earliest Cambrian orogenic events. All samples showing U-Pb detrital zircon age spectra with peaks at 650–570 Ma carry relatively large amounts of zircon grains with juvenile Hf isotope characteristics, i.e. positive εHf(t) (up to +10) suggesting their derivation from continental or Island arcs. The presence of exotic tectonic blocks composed of Ediacaran arc-type rocks hosted by the accretionary complex of the South Tienshan suggests that an extended arc system once existed at the southern convergent margin of the Turkestan Ocean. That arc system provided clastic material for the Palaeozoic sediments of the South Tienshan, but was probably destroyed by tectonic erosion during early Palaeozoic oceanic subduction.

1. Introduction

The Central Asian Orogenic Belt (CAOB) is the world largest accretionary orogen comprising numerous Precambrian to Palaeozoic continental blocks and Island arcs that amalgamated as a result of the suturing and final closure of the Paleo-Asian Ocean during the late Palaeozoic (e.g. Zonenshain *et al*. 1990; Windley *et al*. 2007; Biske and Seltmann 2010; Safonova *et al*. 2011; Xiao *et al*. 2013; Kröner *et al*. 2014). In the southern

part of the CAOB, the late Palaeozoic events formed the South Tienshan collisional orogenic belt, which is critically important for understanding the evolution of the CAOB as a whole. The South Tienshan formed as a result of the suturing of the Turkestan Ocean and other branches of the Paleo-Asian Ocean and convergence and collision between ancient continental blocks of the Paleo-Kazakhstan in the north and the Karakum and Tarim continents in the south (Figure 1) (e.g. Biske
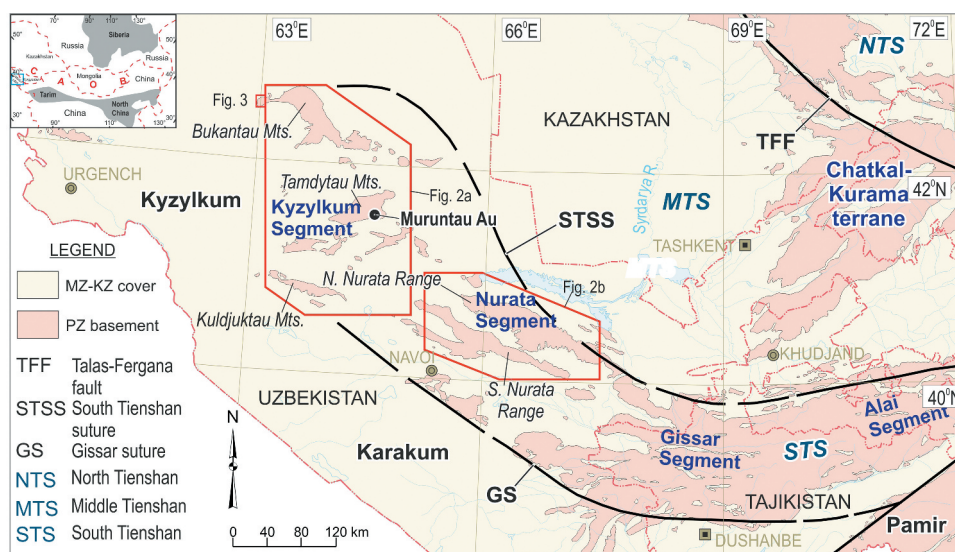
Figure 1. Major tectonic units of the western Tienshan (modified from Dolgopolova *et al*. 2017).

1996; Windley *et al*. 2007; Biske and Seltmann 2010; Burtman 2015; Safonova *et al*. 2016). The evolution of the Tarim margins has been relatively well studied (e.g. Xiao *et al*. 2013; Zhang *et al*. 2013, 2019; Wang *et al*. 2018), however, we know much less about the Neoproterozoic and Palaeozoic evolution of the westernmost Tienshan belt built up on the basement of the Karakum continent. Unlike the Tarim marginal terranes, the western South Tienshan and Karakum include Palaeozoic suture zones dissecting the northern Karakum margin. These suture zones separate microcontinents, the northern Karakum margin and accretionary complexes of the South Tienshan exposed in the territory of western Uzbekistan (e.g. Biske and Seltmann 2010; Dolgopolova *et al*. 2017; Savchuk *et al*. 2018; Konopelko *et al*. 2019). These terranes occupy vast areas of ca. 1000 × 1000 km and are covered by sands of the Kyzylkum and Karakum deserts (Figure 1). Consequently, their geodynamic evolution remains poorly understood, in particular, in terms of the ages, provenances and depositional environments of fossil-free siliciclastic formations. Few, if any, U-Pb detrital zircon ages and Hf-in-zircon isotopes and up-to-date whole-rock and geochemical data from those clastic sedimentary formations have been reported so far. The only three samples of clastic sediments of the lower allochthon and upper allochthon (Besapan 3 Fm.) collected in the southeastern and central Kyzylkum Desert have been analysed for U-Pb detrital zircon ages before (Mirkamalov *et al*. 2012; Konopelko *et al*. 2019). However, no chemical data from such rocks have been reported so far. Those three samples show similar maximum depositional ages of 580–520 Ma suggesting that they were

derived from provenances consisting of coeval igneous formations. To fill that gap and to make geochronological and geodynamic constrains more reliable, in this paper we present first results of geochemical, isotopic (whole-rock Nd and Hf-in-zircon) data and new U-Pb detrital zircon ages from nine samples of Neoproterozoic to early Palaeozoic fossil-free clastic sedimentary rocks sampled in the Bukantau and Tamdytau of the Kyzylkum Desert and in the Northern Nuratau Mts. (Figure 1). We will focus on the composition and depositional ages of clastic sediments in an attempt to reconstruct tectonic settings of their deposition and to provide more details on the composition and nature of their igneous protoliths.

2. Regional tectonic outline and geology

2.1 Major tectonic units of the western Tienshan

The western Tienshan in the territory of Kyrgyzstan, Tajikistan and Uzbekistan consists of three major tectonic units or terranes: Northern Tienshan, Middle Tienshan and South Tienshan (Zonenshain *et al*. 1990; Biske and Seltmann 2010; Burtman 2015). These east-west trending linear terranes are cut by the NW trending Talas-Fergana Fault with a total dextral offset of about 200 km (Figure 1). The Northern Tienshan represents an early Palaeozoic continental arc formed at the southern margin of the Paleo-Kazakhstan continent as a result of the northward subduction and subsequent closure of the Terskey Ocean during the late Ordovician (Lomize *et al*. 1997; Ghes 2008). The Middle Tienshan includes the Chatkal-Kurama terrane, a late Palaeozoic continental arc formed during the

evolution and closure of the Turkestan Ocean, a branch of the Paleo-Asian Ocean separating the Paleo-Kazakhstan from the southern continents of Karakum and Tarim (Biske and Seltmann 2010; Safonova *et al*. 2016). The Middle and South Tienshan are separated by the Southern Tienshan Suture. The South Tienshan belt represents an accretion-collisionak belt or a pile of folded tectonic nappes, which were thrust southward over the passive margin of the Karakum-Tarim continent during the closure of the Turkestan Ocean in late Carboniferous time (Biske and Seltmann 2010). It also hosts shelf limestones of the Kyzylkum-Alai terrane that was accreted to an active margin of the Turkestan Ocean in the Silurian. The western part of the South Tienshan consists of four segments (west to east): Kyzylkum, Nurata, Gissar and Alai (Figure 1). In this paper, we focus on the Kyzylkum andNurata segments.

2.2 Geology of the Kyzylkum Desert area and sampling sites

The Palaeozoic formations exposed in the Kyzylkum Desert and in the Nurata Range constitute the Kyzylkum and Nurata segments of the South Tienshan terrane. The Kyzylkum and Nurata segments compose a large accretion-collisional complex formed in a late stage of the evolution of the Turkestan Ocean, at an active margin of the Paleo-Kazakhstan continent (Figure 1) (Burtman 1975; Mukhin *et al*. 1988; Biske and Seltmann 2010; Savchuk *et al*. 2018). The South Tienshan terrane is bounded from the north by the Southern Tienshan Ophiolite Suture zone. The ophiolites of the suture zone crop out in the northern Nuratau Range and can be traced under the Mesozoic–Cenozoic sediments of the northern Kyzylkum Desert. A metagabbro sampled in the Northern Nuratau Range yielded a U-Pb zircon age of ca. 448 Ma (Mirkamalov *et al*. 2012). The southern boundary of the South Tienshan terrane and the adjacent Karakum active margin include several Palaeozoic sutures, e.g. Ordovician metavolcanic rocks of the Kuldzhuktau Mts. and serpentinites of the southern Nuratau Range (Biske and Seltmann 2010). The metamorphic rocks exposed in the northern Nuratau Range may represent fragments of the basement of the South Tienshan terrane (e.g. Akhmedov 2000), however, they are not exposed outside the Nuratau Range. The U-Pb ages of igneous zircons from Palaeozoic granites (Chiaradia *et al*. 2006) and detrital zircons from metasediments (Seltmann *et al*. 2011; Mirkamalov *et al*. 2012; Konopelko *et al*. 2019) suggest that the basement of the Kyzylkum and Nurata segments is Neoproterozoic,

although the ca. 2.5 Ga detrital zircons indicate the presence of Archaean to Paleoproterozoic rocks in the provenance.

The Kyzylkum Desert and the Northern Nuratau Range are dominated by latest Neoproterozoic – early Palaeozoic clastic sediments forming a Caledonian turbidite-type complex (Figures. 2, 3) (Biske 1996). The complex consists of variable metamorphosed sedimentary formations of two allochtonous units: lower and upper (Mukhin *et al*. 1988). The lower allochthon unit includes (bottom to top) quartzites, amphibolites and schists of the Taskazgan Formation, sandstones and shales of the Besapan 1 Formation and shales and turbidites of the Besapan 2 Formation also referred to as 'black Besapan' (Bukharin *et al*. 1985). The upper allochthon unit includes (bottom to top) flyschoids with carbonate and siliceous olistolithes of the Besapan 3 Formation also referred to as 'variegated Besapan' and rhythmically bedded clastic sediments of the Besapan 4 Formation also referred to as 'green Besapan' (Bukharin *et al*. 1985; Akhmedov *et al*. 2001). According to the Stratigraphic Code of Uzbekistan, these four 'Besapans" must be referred to as Kurgantau Fm., Rokhat Fm., Kosmanachi Unit, and Murun Fm., respectively (Akhmedov *et al*. 2001). In general, the Besapan and Taskazgan formations are tectonically juxtaposed in extended mélange zones (Mukhin *et al*. 1988; Savchuk *et al*. 1991). The rhythmically bedded black shales host several prominent Au deposits including the world known giant Muruntau Au-deposit hosted by Besapan 3 Fm. shales (Glorie *et al*. 2019; Seltmann *et al*. 2020).

In the northern Kyzylkum (Figure 2(a)), the sedimentary and volcanic rocks exposed in the Bukantau Mts. belong to the Baimen Fm. of lower-middle Llandovery age (graptolites; Akhmedov *et al*. 2001), consisting of rhythmically interbedded siliceous mudstone, siltstone and shale with sandstones (Figure 3). In the central Kyzylkum (Figure 2(b)), the turbiditic packages associated with oceanic sediments and siliceous shales and mafic to andesitic volcanic rocks belong to the Kaltadavan Fm. of middle to late Ordovician age determined by conodonts and chitinozoans (Akhmedov *et al*. 2001). However, Biske and co-authors think that those age constrains are erroneous as come from an allochtonous tectonic sheet thrust under a package of sandstones carrying zircons which youngest ages are Cambrian (Biske *et al*. 2021). The Kaltadavan Fm. is exposed only in the northern Nuratau and western Turkestan ranges and probably is an analogue of the Besapan and Taskazgan formations of the northern Kyzylkum composing the lower allochthon.
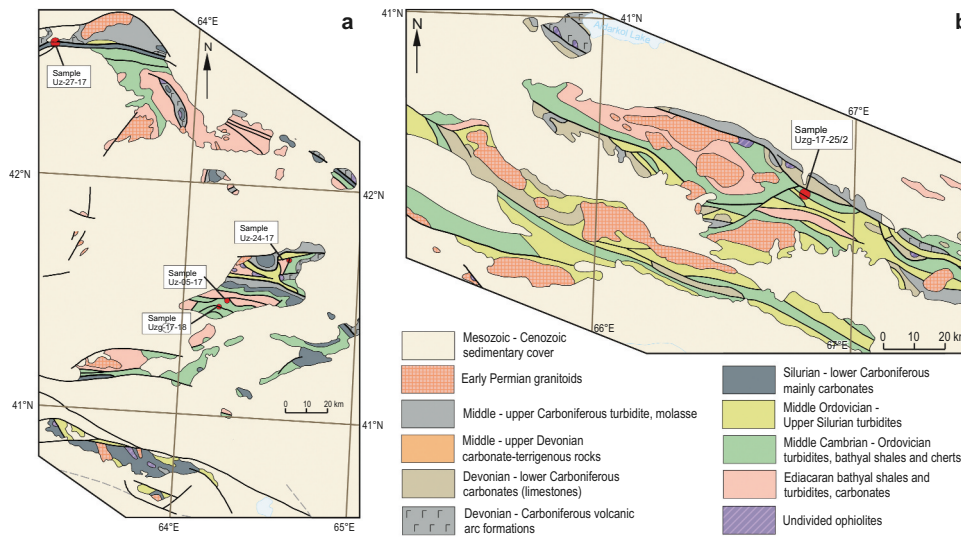
Figure 2. Geological sketch maps of the Kyzylkum and Nurata segments: A, Tamdy and Bukantau mts., Northern Kyzylkum; B, Nurata Mts., showing sampling locations.
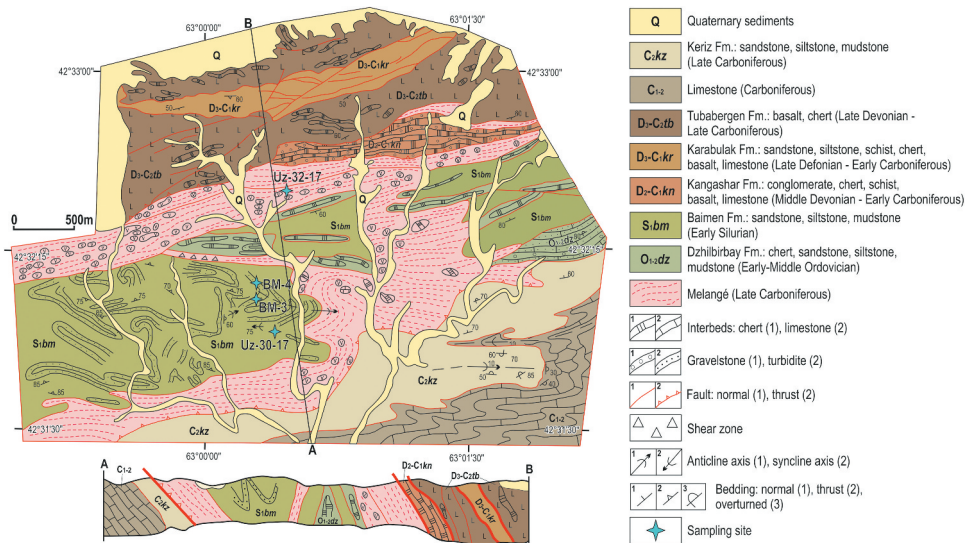
Figure 3. Geological sketch map of the Baimen site in the Bukantau Mts. showing the location of samples. Note that ocean plate stratigraphy lithologies belong to the Dzhilbirbay (early-middle Ordovician) and Baimen (early Silurian) formations and they also occur as blocks in melange.

In this paper, we present first U–Pb ages and geochemical data from nine samples of sandstones collected at several localities of the northern and central Kyzylkum (Figures 1– 3). For sampling coordinates and sample description see Supplementary table S1. All sampled sandstones come from turbidite-type packages associated with ocean plate stratigraphy lithologies (Isozaki *et al*. 1990; Safonova *et al*. 2016): pillowed basalt, pelagic chert and hemipelagic siliceous mudstone and siltstone and turbiditic sandstone (Figure 4). Note, that clastic

sediments, typically sandstones of accretionary complexes, may belong to both ocean plate stratigraphy trench sequence and cover overriding plate cover sequence.

Sandstone sample UZG-17-18 was collected from a rhythmic sedimentary sequence of the Besapan 2 Fm. of the lower allochthon, approximately 8 km south of the Muruntau Au deposit of the Tamdy Mts. in the northern Kyzylkum Figure 2(a), 5(a). Sample Uz-24-17 was collected in a mélange zone in the northern Tamdy Mts. and also

Figure 4. Field photos of ocean plate stratigraphy and supra-subduction lithologies all typical of subduction-accretionary complexes: pelagic chert, pillow basalt, and volcanic flows from the Tamdy (A-D) and Bukantau (E-F) mountains. A, C, E, chert; B, D, pillow lavas; F – volcanic rocks.

probably represents a sedimentary formation of the lower allochthon (Figure 2(a)). Sample Uz-05-17 of the Besapan 4 Fm., the upper allochthon, was collected in the southern Tamdy Mts. Figure 2(a), 5(b). Five more samples of sandstones (Uz-27-17, Uz-30-17, Uz-32-17, BM-3, BM-4; Figure 5(c)) of the Baimen Fm. were collected in the Bukantau Mts., the northernmost part of the study area (Figure 2(a), 3). Sample UZG-17-25/2 is a sandstone of the Kaltadavan Fm. collected in the northern Nuratau Range (Figure 2(b)).

3. Petrography

Figure 6 shows microphotographs of thin sections of the sandstones under study. Sample BM-3 belongs to the Baimen Fm. of Silurian age and was collected in the western Bukantau Mts. (Figure 3). The moderately sorted greenish-grey fine-grained (0.1–0.25 mm) sandstone consists of angular to sub-rounded grains of mono- and polycrystalline quartz (50%), plagioclase

(less than 10%), lithic fragments of quartzite, siliceous and volcanic rocks (30%), muscovite and biotite (2%). The cement contains clay minerals (Figure 6(a)).

Sample Uz-05-17 belongs to the green Besapan 4 Fm. and was collected in the southern Tamdy Mts. (Figure 2(a)). The poorly sorted greenish silty sandstone consists of angular and sub-rounded mono- and polycrystalline quartz (50%), plagioclase (5%) and muscovite (2%). The cement consists of secondary quartz (Figure 6(b)).

Sample Uzg-17-18 was collected in the northern Tamdy Mts. from a package of interbedded siltstone and sandstone of the lower part of the Besapan Fm. (Figure 2(a)). The grey fine/medium-grained (0.1-.04 mm) poorly sorted silty sandstone is dominated by mono- and polycrystalline quartz with subordinate plagioclase and muscovite and accessory zircon. The cement consists of clay minerals Figure 6(c,d).

Sample Uzg-17-25/2 was collected in the northern Nuratau Mts. from a package of medium/coarse-grained sandstones of the Kaltadavan Fm. (Figure 2

Figure 5. Outcrop photographs of sandstones from the Besapan 2 Fm. (a) and Besapan 4 Fm. (b) of the Tamdy Mts., Baimen Fm. of the Bukantau Mts. (c) and Kaltadavan Fm. of the northern Nuratau Mts. (d).
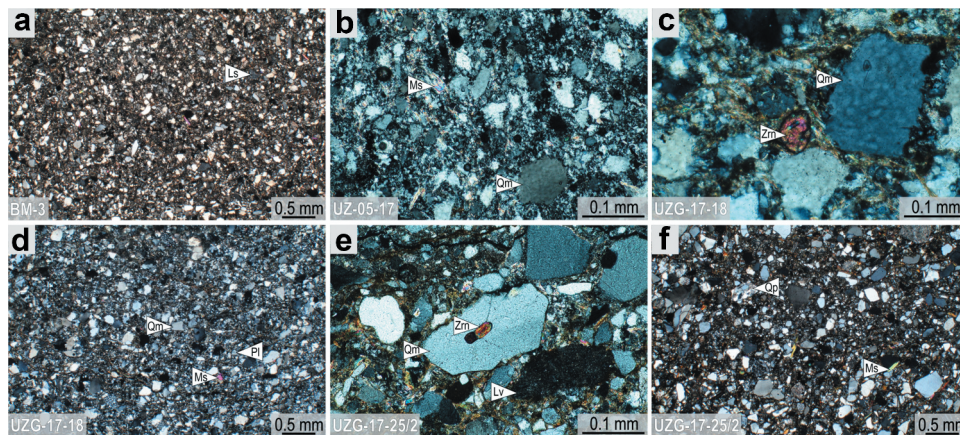
Figure 6. Microphotographs of thin-sections of Kyzylkum-Nurata sandstones (crossed nicoles). Abbreviations: Ls – lithic fragments of sedimentary rocks, Lv – lithic fragments of volcanic rocks, Ms – muscovite, Pl – plagioclase, Qm – monocrystalline quartz, Qp – polycrystalline quartz, Zrn – zircon.

(b)). The poorly sorted dark grey medium/coarse-grained (0.2–0.8 mm) sandstone consists of sub-angular to rounded grains of mono- and polycrystalline quartz (40%), feldspar (15%), lithic fragments of granoblastic microquartzite, siliceous and volcanic rocks (10%), muscovite and biotite (2%) and accessory zircon (Figure 6(e,f)). The cement consists of chlorite and clay minerals.

For six samples containing less cement we performed petrographic counting to evaluate their model composition (Supplementary table S2). We counted at least 300 grains of lithic rock and mineral fragments (Lv – volcanic, Ls – sedimentary), quartz (Q) and feldspar (F). The petrography-based classifications of Shutov (1967) and Folk (1980) show that all sandstones represent quartz-
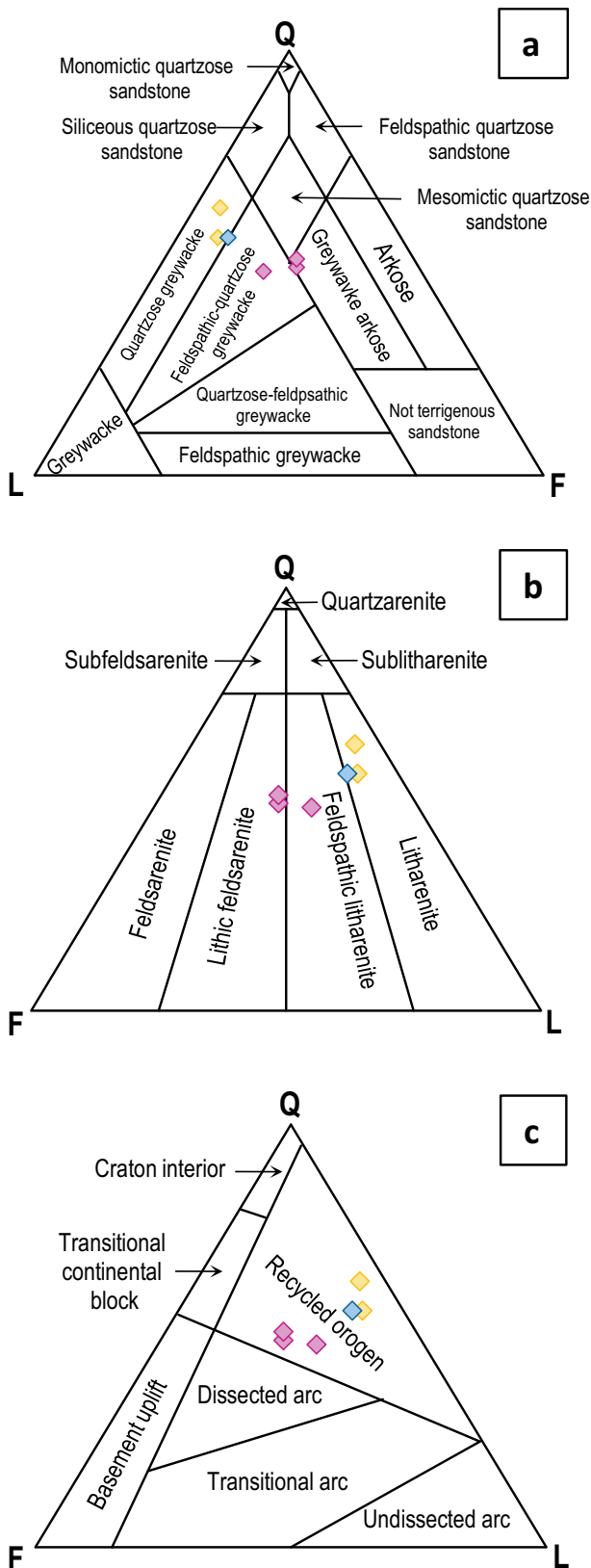
Figure 7. Petrography based classification diagrams: (a), Shutov (1967); (b), Folk (1980); (c), Dickinson *et al*. (1983). L – lithic fragments, Q – quartz, F – feldspar.

feldspar greywackes, quartz greywacke and arkose grey-wacke (Shutov 1967) and litharenite, feldspatic lithare-nite and lithic felsarenite, respectively (Folk 1980) (Figure 7).

4. Results

In order to reconstruct the composition and provenance of the Kyzylkum and Nurata sandstones under study we performed U–Pb isotope dating and Lu-Hf analysis of detrital zircons, whole rock major and trace element ana-lyses and Nd isotope measurements. For details on the methodology and analytical procedures see Electronic supplementary document S1.

4.1. U-Pb detrital zircon geochronology

Zircon grains from the nine samples of sandstones were analysed by LA-ICP-MS at the University of Nanjing, China. The U–Pb analytical data and calculated ages are pre-sented in Supplementary table S3. Following a common practice for further interpretation and discussion, we used the $^{206}Pb/^{238}U$ ratios for the inferred ages younger than 1000 Ma and $^{207}Pb/^{206}Pb$ ratios for zircons older than 1000 Ma (Black and Jagodzinski 2003; Black *et al*. 2003). For sample descriptions see section 2 and Supplementary table S1.

Sample Uzg-17-25/2 (Kaltadavan Fm.) carries slightly elongated and rounded detrital zircon grains, which yielded 71 U-Pb ratios and calculated ages (Figure 8(a)). The calculated U-Pb ages range from 2750 to 542 Ma with two major broad peaks at 2700–2400 and 1200–750 Ma and one younger narrow peak at 564 Ma. In addition, eleven grains yielded sporadic ages in the range of 2200–1600 Ma. Six youngest grains with ages ranging from 598 to 542 Ma suggest a latest Neoproterozoic Ediacaran maximum depositional age of the Kaltadavan Fm. in the Nuratau Mts.

Samples Uz-05-17, Uzg-17-18 and Uz-24-17 (Besapan Fm.) yielded 197 U-Pb ages (Figure 8(b)). The calculated U-Pb ages range from 3080 to 541 Ma with a major broad peak at 1000–550 Ma and a smaller narrow peak at 2500 Ma. The remained ages are in the range of 2300–1500 Ma and two grains yielded Archaean ages of ca. 3000 Ma. The youngest 14 grains in the range from 598 to 541 Ma suggest a latest Neoproterozoic Ediacaran max-imum depositional age of the Besapan Fm. in the Tamdy Mts.

Samples Uz-27-17, Uz-30-17 and Uz-32-17 (Baimen Fm.) yielded similar spectra of U-Pb detrital zircon ages and therefore in Figure 8(c) we show summarized
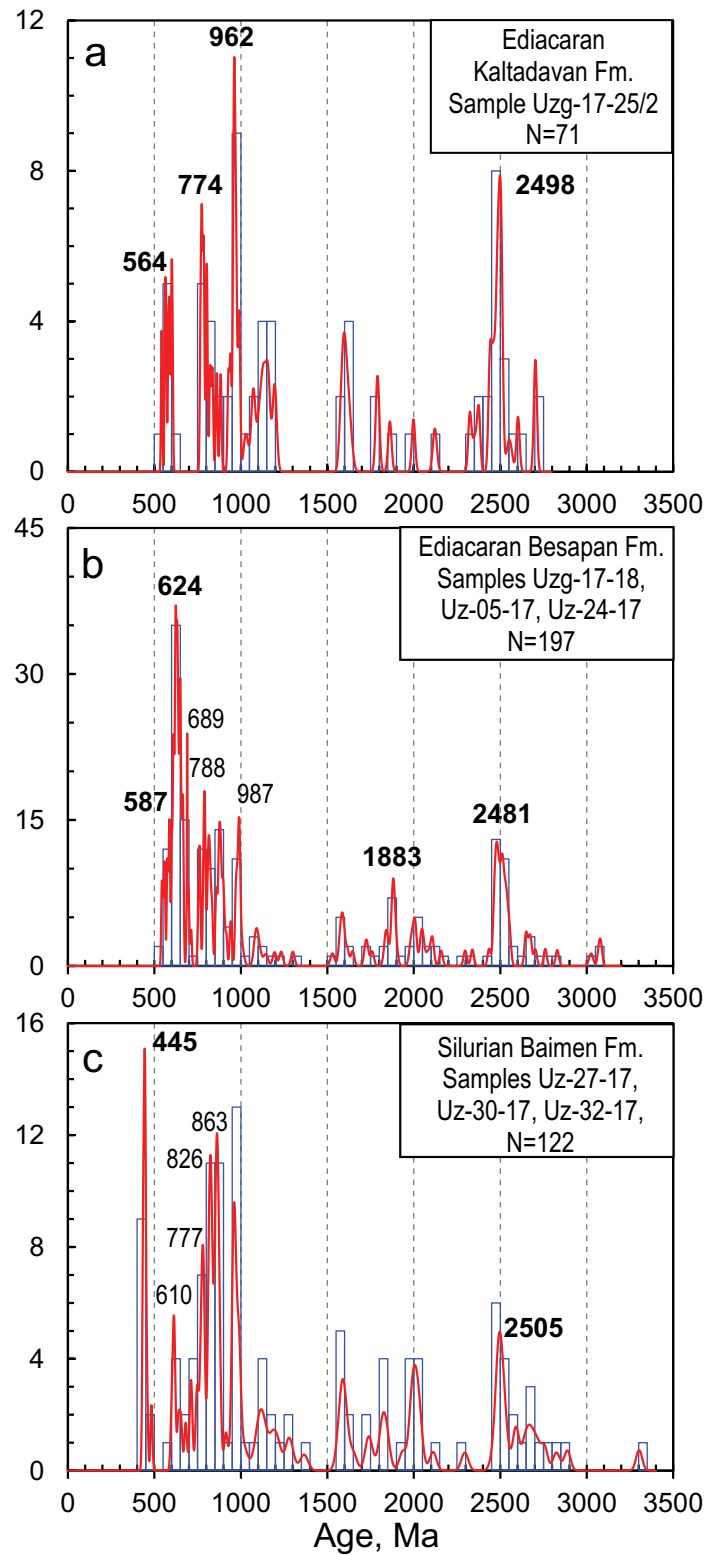
Figure 8. Histograms of U-Pb detrital zircon ages with probability density curves for sandstones of the Kaltadavan (a), Besapan (b) and Baimen (c) formations.

histograms and probability plots. The U-Pb ages range from 3302 to 433 Ma with a broad peak at 1200–600 and a younger narrow peak at 445 Ma. Similar to other

Kyzylkum samples, the Baimen samples show smaller broad peaks at 2800–2400 and 2100–1550 Ma (Figure 8 (c)). The youngest nine grains yielded ages ranging from

450 5 434 Ma suggesting the early Silurian (Llandovery) maximum depositional age of the Baimen Fm. in the Bukantau Mts.

4.2. Whole-rock chemical composition

The whole-rock major and trace element data from the nine samples of sandstones were obtained in the Institute of Geochemistry, SB RAS, Irkutsk, Russia (Supplementary tables S4 and S5). In the classification diagram of Petijohn (1972), seven samples plot in the field of litharenite and two samples plot in the field of greywacke (Figure 9(a)). The analysed sandstones have high concentrations of SiO_2 in the range of 72 to 84 wt. %, which are higher than that of the average upper continental crust (UCC; 66.6 wt. %) and post-Archaean Australian shales (PAAS; 62.4 wt. %) (Taylor and McLennan 1985). Accordingly, the concentrations of other major oxides are lower than in the UCC and PAAS and generally demonstrate negative correlations with SiO_2 in variation diagrams (Supplementary figure S1). To evaluate paleoweathering or recycling conditions of sediment deposition we used popular indexes of CIA (chemical index of alteration) and ICV (index of compositional variability) (Figure 9(b)) (Nesbitt and Young 1982; Cox et al. 1995; Cullers and Podkovyrov 2000). High CIA values typically suggest strong weathering because the CIA values for unaltered plagioclase and K-feldspar are around 50, whereas those of kaolinite and gibbsite-rich shales, the products of strong weathering, are close to 100 (Nesbitt and Young 1982, 1984). The sandstones have CIA in the range close to that of PAAS or slightly lower (CIA = 67.6–72.3) implying a provenance dominated by strongly weathered sources with a possible minor participation of weakly weathered sources in

several samples (Figure 9(b)). In general, the CIA indexes accord well with the general desert environment of sandstones.

ICV values reflect the compositional maturity of source rocks (Cox et al. 1995; Cullers and Podkovyrov 2000). Low ICV values commonly indicate a mature source with abundant clay minerals typical of passive margin or continental settings, whereas high ICV values generally imply an immature source typical of active margin settings. The analysed sandstones have ICV values in a narrow range of 0.95 to 1.2 (Figure 9(b)), i.e. slightly higher than the ICV of PAAS (0.84) suggesting a mature detrital source in the provenance with a possible participation of immature sources such as intra-oceanic arcs and/or active continental margins.

Concentrations of trace elements in sediments generally reflect the composition of protolithic igneous sources once dominated in provenance. Large-ion lithophile elements (LILE), e.g. K, Na, Rb and Sr, can be mobile during sedimentation and/or metamorphism and, therefore are of little significance in determining source characteristics. The rare-earth elements (REE) and high-field strength elements (HFSE) and their ratios (e.g. La/Th) are more stable during sedimentation and may reflect chemical differentiation in terrigenous sedimentary rocks. Mature and fine-grained clastic sediments such as PAAS (Nance and Taylor 1976) tend to have higher abundances of La, Th, U, Zr and Hf and lower abundances of Ti, V, Co, Sc and Y compared to immature poorly sorted sediments such as Island arc greywackes (Taylor and McLennan 1985; Condie 1993). In addition, the REE have very low solubility in water and seldom fractionate relative to each other during exogenous processes. Therefore, REE abundances and normalized patterns should reflect compositions of source areas (McLennan 1989; Condie 1993).
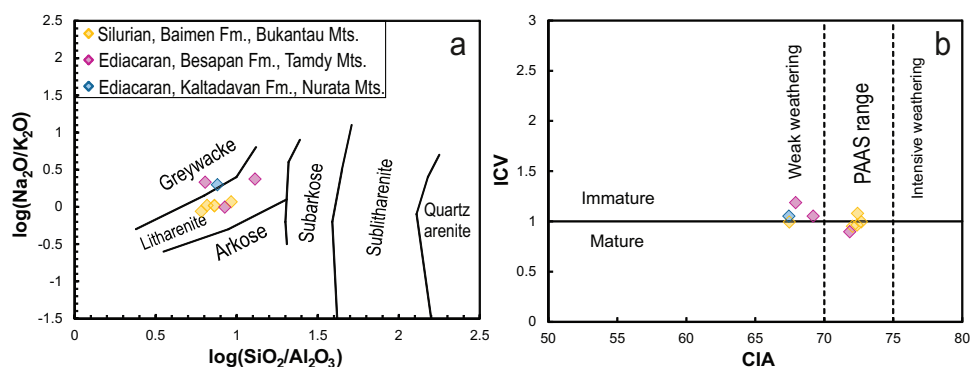
Figure 9. Classification diagrams: (a) log(Na_2O/K_2O) vs. log(SiO_2/Al_2O_3) (Petijohn, 1972) and (b) ICV vs. CIA for Kyzylkum-Nurata sandstones. The index of chemical alteration, CIA = [$Al_2O_3/(Al_2O_3+ CaO*+Na_2O+K_2O)$] ×100, where CaO* is the content of CaO in silicate minerals only, is given after (Nesbitt and Young 1984) and the Index of Compositional Variability, ICV = ($CaO+K_2O +Na_2O+Fe_2O_3+ MgO + MnO +TiO_2)/Al_2O_3$ is given after (Cox et al. 1995).
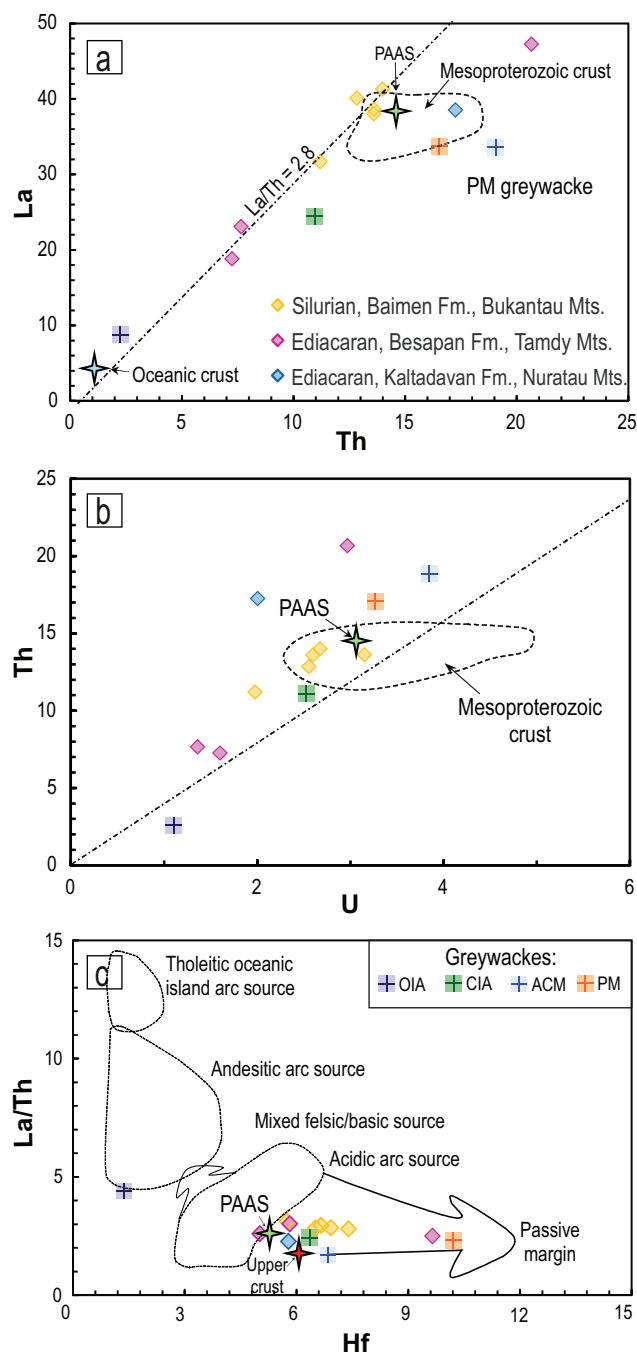
Figure 10. Discrimination diagrams: A, La vs. Th; B, Th vs. U; C, La/Th vs. Hf after (Floyd and Leveridge 1987). Sources: (Zhao *et al.* 1993) (Mesoproterozoic crust), (Taylor and McLennan 1985) (PAAS), Bhatia et al., 1986 for average greywacke compositions (OIA, oceanic Island arc; CIA, continental Island arc; ACM, active continental margin; PM, passive margin.

In the La–Th and Th–U diagrams Figure 10(a,b), most sandstones plot in the field of the Mesoproterozoic crust and close to PAAS with affinities to the average composition of greywacke from continental magmatic arcs suggesting their derivation from older continental

crust. However, two samples of sandstones from the Besapan Fm. plot between the PAAS and oceanic crust suggesting participation of intra-oceanic arc sources. In addition, discrimination diagram La/Th – Hf uses Hf as a proxy to distinguish sediments formed in a passive margin environment due to the accumulation of Hf-rich minerals, such as zircon, in mature sediments. In the La/Th – Hf diagram, most sandstones plot close to the average composition of the upper crust with a trend towards the field of passive margin, while one sample of the Besapan Fm. plots in the field of acidic arc sources (Figure 10(c)).

Figure 11 shows the chondrite-normalized and PAAS normalized REE patterns of the sandstones in comparison with that of PAAS Figure 11(a,c). The chondrite-normalized REE patterns of the analysed sandstones are characterized by Eu anomalies typical of igneous rocks with plagioclase fractionation, e.g. andesitic lavas of intra-oceanic or continental arcs. The PAAS-normalized REE patterns are parallel to that of PAAS aligned both above and below the PAAS line. The primitive mantle normalized multi-element patterns of the Kyzylkum-Nurata sandstones are similar to that of PAAS but at higher levels and are characterized by negative Nb-Ta and Ti anomalies typical of supra-subduction lavas (Figure 11(b)). The PAAS normalized multi-element patterns of the Kyzylkum-Nurata sandstones are much more different from the PAAS pattern though as they show troughs at K, Sr and Ti and peaks at Zr-Hf.

4.3. Whole-rock Nd isotopes

Nd isotopic characteristics of sediments are indicative of their sources due to the low mobility of the REE. In this paper, we present first Sm–Nd isotopic data from seven whole-rock samples of the sandstones. The Sm–Nd isotope ratios were measured in the Geological Institute of the Kola Science Center, Apatity, Russia. The isotope data are illustrated by an isotope evolution diagram in Figure 12(a). The initial isotopic ratios were calculated using the depositional ages obtained in this study (Supplementary tables S3 and S6; Figure 8).

The sandstones show variable and negative εNd(t) values ranging from – 6.5 to – 16.3. The Silurian sandstones of the Baimen Fm. are characterized by the largest variations and the lowest εNd(t) values (–16.3) (Figure 12(a)). Three samples of these rocks have εNd(t) values – 8.5, – 10.0 and – 16.3 with crustal Nd model ages (T_{DM}*) 1.9, 2.0 and 2.5 Ga, respectively. In the Nd evolution diagram (Figure 12(a)), the Nd isotope data plot in the fields of middle-early Proterozoic and late Archaean crust suggesting the presence of recycled Precambrian

continental crust in the provenance. More evidence for this comes from the Nd model ages ranging from 2.5 to 1.9 Ga, i.e. much older than the ca. 0.45 Ga depositional ages of the sandstones and from the large amount of Archaean and earliest Proterozoic detrital zircons (Supplementary table S3, Figure 8).

The Ediacaran sandstone of the Kaltadavan Fm. (Uzg-17-25/2) also has a strongly negative value of εNd(t), −14.8, and a very old crustal Nd model age of 2.5 Ga. In the Nd evolution diagram (Figure 12(a)), it plots in the field of late Archaean crust. The histogram shows a large number of Archaean and earliest Proterozoic detrital zircon grains, similar to that of the Baimen samples (Supplementary table S3), Figure 8(a,c).

Three samples of Ediacaran sandstones of the Tamdy Mts. have slightly higher εNd(t) values of − 6.5, − 8.8 and − 9.4 with crustal Nd model ages TDM* of 1.8, 2.0 and 2.1 Ga, respectively. In the Nd evolution diagram, the samples plot in the field of middle-early Proterozoic crust suggesting derivation from recycled Precambrian continental crust. However, one sample has a slightly higher εNd(t) value compared to the Baimen (Silurian) and Kaltadavan (Ediacaran) samples. This may be indicative of the presence of juvenile material in the provenance of the Besapan sandstones. More evidence for this comes from their geochemical characteristics, which are transitional between continental and Island arc grey-wackes Figures 10, 12(a).

4.4. Hf-in-zircon isotopes

A number of zircon domains dated by LA-ICP-MS were also analysed for their Lu–Hf isotopic compositions at the University of Hong Kong, China (Supplementary table S7; Figure 12(b)). Due to technical reasons, we analysed zircon grains larger than 200 µm. Most of them appeared Neoproterozoic though. Seventy four Hf isotopic spot analyses of zircon grains from six sandstone samples yielded variable initial $^{176}Hf/^{177}Hf$ ratios corresponding to εHf(t) values ranging from −20 to +10. The calculate values of εHf(t) suggest compositionally diverse provenances including both ancient continental crust and juvenile sources. The Baimen (Silurian) and Kaltadavan (Ediacaran) sandstones carry zircons with mostly crustal Hf isotope characteristics (εHf(t) < 0). The Besapan samples from Tamdy Mts. (Ediacaran) show a significant proportion of detrital zircons with mixed (0 < εHf(t) < +5) to juvenile (εHf(t) > +5) isotope characteristics with much younger crustal model ages (tHfc) of 1.2–0.9 Ga (Figure 12(b)).

5. Discussion

In this paper, we presented first whole-rock geochemical and Nd isotope data (Figure 9–12a) from sandstones of the southern Tienshan (Figure 1), new U-Pb ages (Figures 8, 13) from Ediacaran-Cambrian sandstones of the Tamdytau Mts. (Kyzylkum segment; Figure 2(a)) and
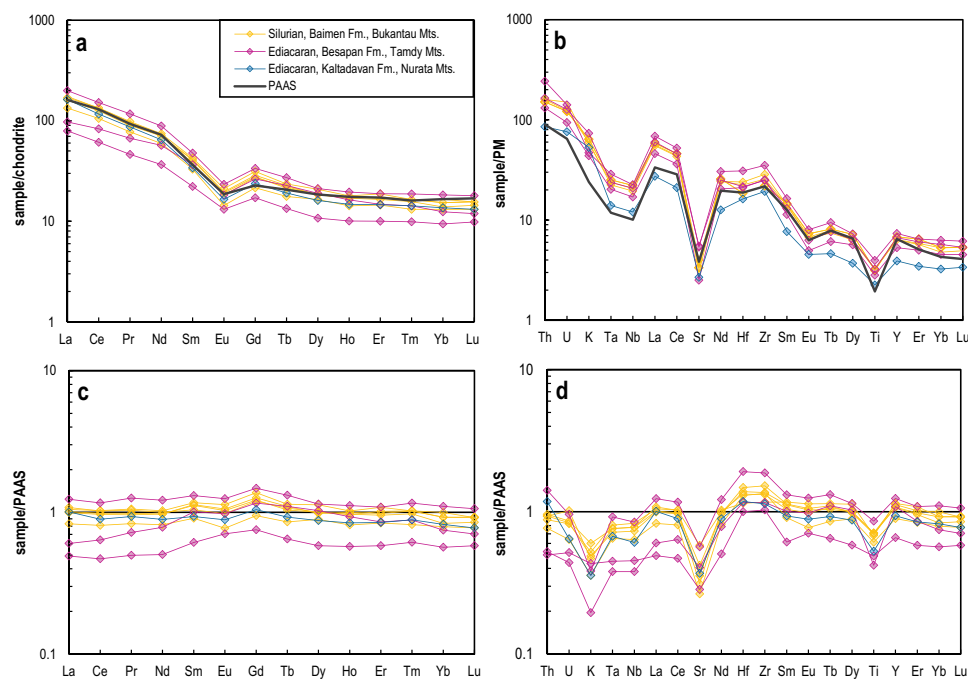
Figure 11. Chondrite-normalized and PAAS normalized REE patterns (A, C) and primitive mantle (PM) normalized and PAAS normalized trace element patterns (B, D) for Kyzylkum-Nurata sandstones. The values of PAAS are from (Taylor and McLennan 1985) and the PM and chondrite normalizing values are from (Sun and McDonough 1989).
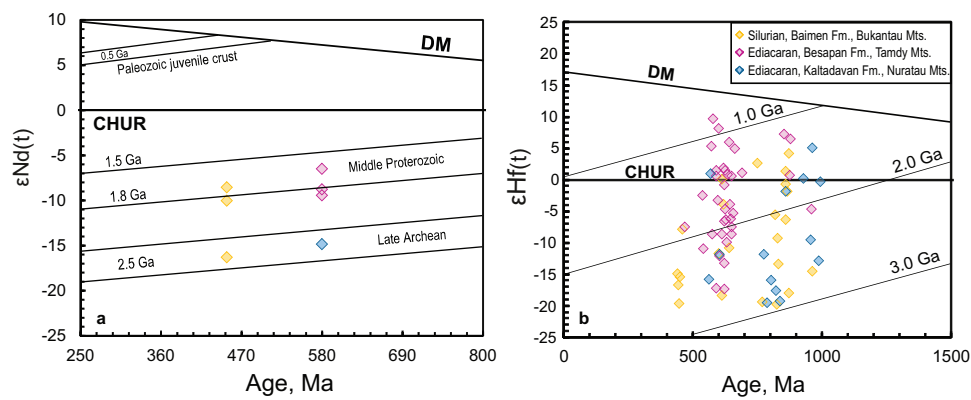
Figure 12. A, Nd isotope evolution diagram for the Kyzylkum-Nurata sandstones; the values of epsilon Nd are calculated based on the depositional ages (Supplementary tables 3 and 6). B, Hf-in-zircon isotope characteristics of the Kyzylkum-Nurata sandstones; the values of εHf(t) were calculated based on the U-Pb ages of individual zircon grains.

Northern Nuratau Mts. (Nurata segment; Figure 2(b)) and first detrital zircon data from the Silurian sandstones of the Bukantau Mts. (Figure 3). Among those are first Hf-in-zircon data from sandstones of the whole Uzbek Tienshan (Figure. 12(b), 15). In this section, we discuss all new and previous zircon and whole-rock data from the Kyzylkum-Nurata sandstones in terms of their depositional ages (Figures. 8, 13), probable provenances (Figure 14), age and nature of igneous protoliths (Figures. 13, 15) and geodynamic environments reconstructed for the study area and the whole southern Tienshan (Figure 16).

5.1. Depositional ages and implications for the pre-Devonian stratigraphy of Kyzylkum-Nurata

In that region, there are only tectonic slices of Ordovician and Silurian turbidites also known as a Caledonian clastic turbidite-type complex, overlapped by Devonian-Carboniferous limestones (Figures 1–3, 5). Based on lithology and conditions of metamorphism, previous researchers traditionally divided those metasediments into several formations varying in ages from the Riphean for quartzites and amphibolites of the Taskazgan Fm. to the late Ordovician for the flyschoids of the upper Besapan Fm. (Akhmedov 2000). However, recent U-Pb geochronological data did not confirm that stratigraphic pattern (Figures. 8, 13). The youngest U-Pb ages of zircons from most 'Riphean' metamorphic rocks appeared in the range of ca. 560–525 Ma, i.e. latest Ediacaran – earliest Cambrian: 568 Ma for amphibolite (Mirkamalov et al. 2012) and 540–520 Ma for mica schists (Konopelko et al. 2019) from the Taskazgan Fm., and 570–540 Ma for sandstones of the Besapan 1 Fm. (this study; Figure 8). The depositional ages for the less metamorphosed sandstones appeared in the same range: ca.

525 Ma (Besapan 3 Fm.; Mirkamalov et al. 2012), 570–560 Ma (Besapan 4 Fm.; this study) and 560–540 Ma (Kaltadavan Fm., this study) (Figure 8). Similar depositional ages in the range of 580–540 Ma were reported for metasediments of the Fan-Karategin or Yagnob greenschist belt (Konopelko et al. 2015; Käßner et al. 2017; Worthington et al. 2017; Biske et al. 2021) of the Uzbek and Tajik South Tienshan, i.e. 500–1000 km further to the south-east (Figure 1). In general, all the U-Pb detrital zircon age spectra obtained from Kyzylkum-Nurata sediments and metasediments show depositional ages in the range of 570 to 520 Ma with the only exception of a depositional age of ca. 610 Ma (Konopelko et al. 2019) (Figure 13).

Thus, the previous and new data on the depositional ages of Kyzylkum sediments and metasediments indicate that a major part of the Caledonian clastic turbidite-type complex formed during a relatively narrow time interval of 50–70 Myrs, i.e. from the latest Neoproterozoic (Ediacaran) to the earliest Cambrian. In addition, structural and lithological studies show that the sandstones of the Besapan 3 Fm. sampled in the Tamdy Mts., near the Muruntau Au deposit, appeared lithologically identical to those of the lowermost Taskazgan Fm. Therefore, the Besapan 3 and Taskazgan units probably were tectonically juxtaposed in tectonic mélanges (Mukhin et al. 1991; Savchuk et al. 2018). Therefore, we think that the 'visual' traditional Ediacaran stratigraphy of the Kyzylkum segment is actually a tectonic juxtaposition of practically coeval sedimentary successions and/or packages metamorphosed to variable degrees.

The three sandstone samples of the Baimen Fm. (Bukantau Mts.) yielded the youngest detrital zircon U-Pb ages in the ranging from 445 to 433 Ma, which define the depositional ages from the latest Ordovician to the early Silurian (Figure 13). This age interval fits the 448 and 438 Ma U-Pb zircon ages of supra-subduction

ophiolites sampled in the Kyzylkum area (Mirkamalov *et al.* 2012; Dolgopolova *et al.* 2017, respectively). The relatively short periods of sedimentation inferred from the U-Pb zircon ages may imply Pacific-type subduction-related orogeny, which cycle is typically limited by 100 Myrs compared to longer collision-type orogeny (Maruyama *et al.* 2011; Maruyama and Safonova 2019).

5.2 Probable provenances of the sandstones: continent vs. active margin

In general, the U-Pb detrital zircon age curves from the sandstones are similar to those from the Precambrian basement of the Tarim Craton (Rojas-Agramonte *et al.* 2014; Han *et al.* 2015) (Figure 14). Figure 14 also illustrates the probability curves of detrital and magmatic zircon ages from Tarim and Northern Tienshan. The patterns from both, Kyzylkum and Tarim Craton are characterized by a major peak at 1100–750 Ma and additional peaks at around 1800 and 2400 Ma. Similar peaks are also characteristic of the zircon age curves from Northern Tienshan. However, the Grenvillian ages in the range of 1600–1200 Ma form a major peak in the age curves of Northern Tienshan and other terranes of paleo-Kazakhstan (Konopelko and Klemd 2016; Kanygina *et al.* 2021), but are absent in the Tarim age curves. In addition, there are smaller peaks at ca. 1600–1200 Ma ages (Figures 8, 14). Therefore, the paleo-Kazakhstan continents in the north unlikely served sources of clastic material for the sandstones under study.

In Tarim, the detrital zircon age patterns from the early Palaeozoic cover sediments are, in general, similar to those from the Precambrian basement, suggesting the derivation of the sediments from local sources (Han *et al.* 2015). The Karakum continent located south of the South Tienshan and west of Tarim possesses Precambrian basement (Figure 1) (Konopelko *et al.* 2015, 2019; Worthington *et al.* 2017). The sandstones contain significant proportion of late Archaean – early Proterozoic zircons with ages in the range 2700–2400 Ma Figures 8, 12(b). The broad peak at 2700–2400 Ma is also present in the dataset from Tarim. However, in the Tarim age pattern, the Neoarchean peak (2.7–2.4 Ga) is much smaller than the Paleoproterozoic peak (2.0–1.8 Ga) reflecting the major period of magmatism and metamorphism, which formed the core of the Tarim Craton (Zhang *et al.* 2013). On the contrary, the 2.0 Ga peak in the age pattern of the sandstones is much smaller than the Neoarchean peak (Figure 14). Although there are no outcrops of the Kyzylkum basement, which several authors consider as a part of the Kyzylkum-Alai block (Biske *et al.* 2021), we can reconstruct its composition through the ages of detrital zircons hosted by cover sediments, i.e. by the Ediacaran and Silurian sandstones of the Kyzylkum Desert. In general, we argue that the basement of the Kyzylkum segment may consist of Neoproterozoic to early Palaeozoic active margin terranes. After the middle Devonian, the region evolved as a 'true' continent consisting of Caledonian basement covered by middle Devonian-Carboniferous sedimentary cover (Biske *et al.* 2021).
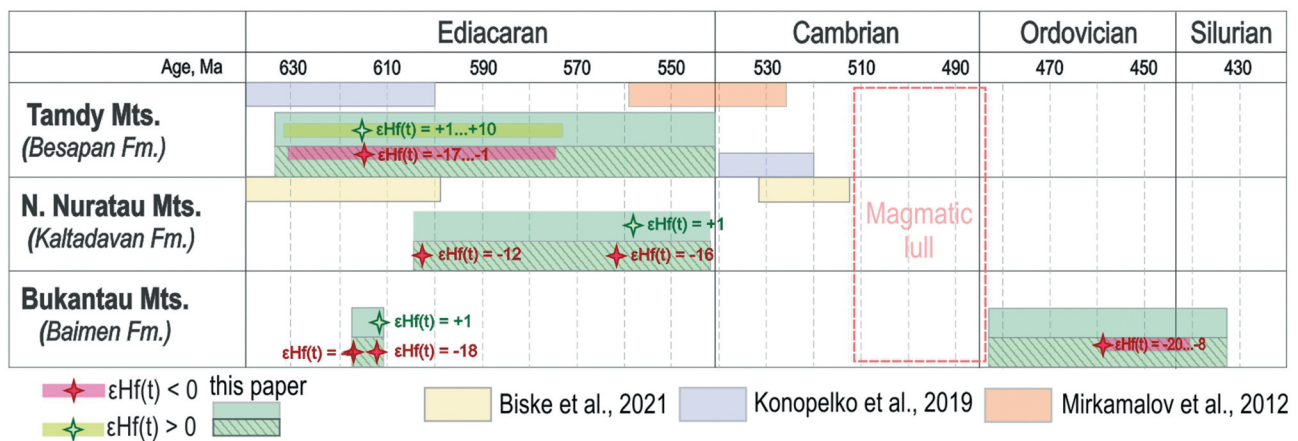
Figure 13. Summary of detrital zircon U-Pb ages (rectangles) and εHf(t) values (bars and stars) obtained from sandstones and metasandstones of the Kyzylkum and Nurata segments and adjacent regions showing two major periods of magmatism in the Ediacaran and Silurian and a magmatic lull in Cambrian time. Green rectangles for the new original U-Pb ages: dashed – dominantly recycled crust; solid – crust with juvenile signatures.
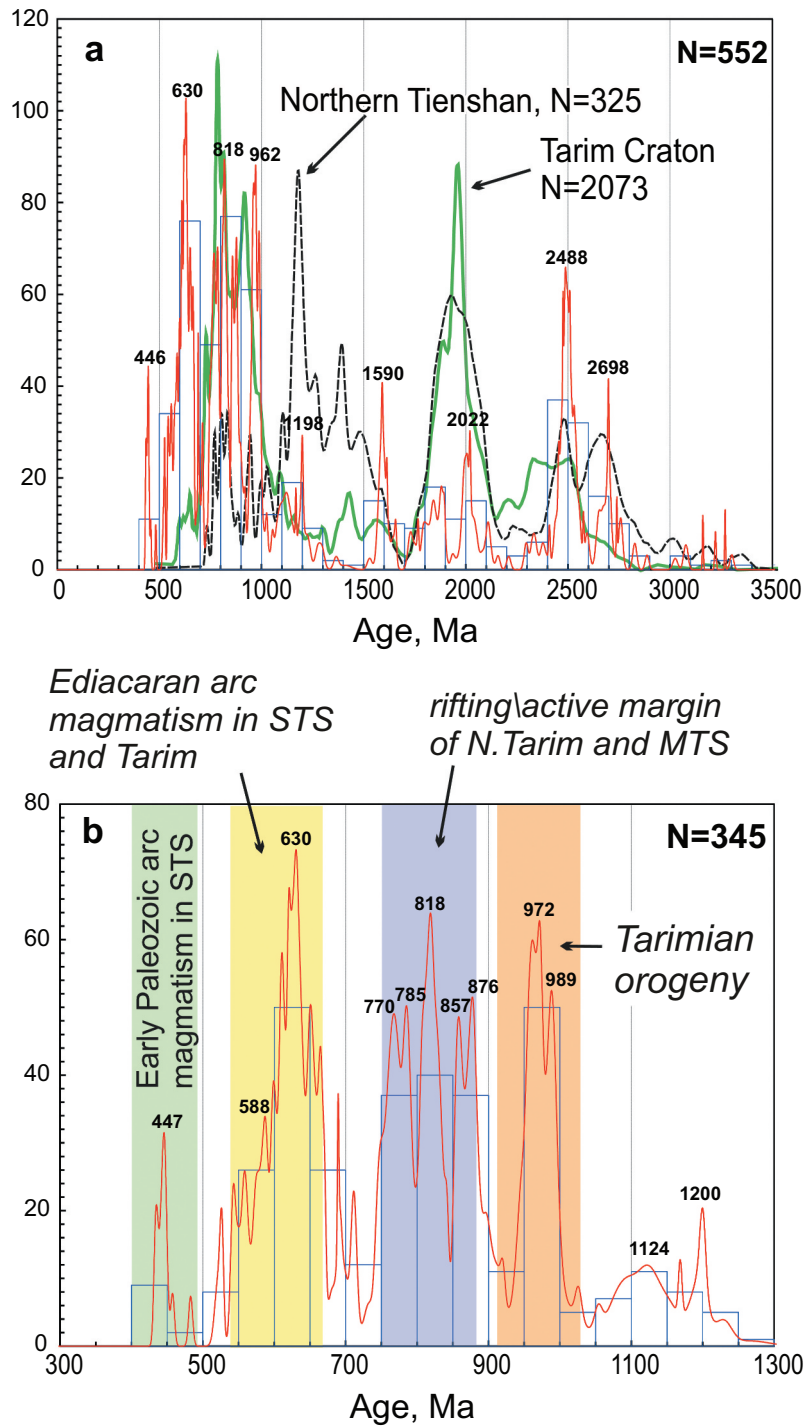
Figure 14. Probability plots with histograms showing the distribution of U-Pb detrital zircon ages from the Kyzylkum-Nurata sandstones (Mirkamalov *et al.* 2012; Konopelko *et al.* 2019; this study): A, compared with those from Tarim and northern Tiehshan; B, with highlighted periods of orogeny and magmatism at 1300–300 Ma. The data from Precambrian and lower Palaeozoic rocks of the Tarim Craton and northern Tienshan (Rojas-Agramonte *et al.* 2014) are shown out of scale. Abbreviations: MTS – Middle Tienshan, STS – South Tienshan.

All Tienshan terranes including the sandstones under study show small amounts of U-Pb detrital zircon ages in the range of 1700–1550 Ma (Figure 14), although no igneous or metamorphic events has been recorded for that time period in any cratonic block south of the Tienshan (Rojas-Agramonte *et al*. 2014). The 1050–900 Ma event of Tarimian orogeny corresponds to the period of calc-alkaline arc-type volcanism well documented by U-Pb zircon age data from both Tarim and Kyzylkum-Nurata sandstones. The prominent peaks at 870–730 and 650–570 Ma are typical of the sandstones under study, whereas the peak of 870–730 Ma is typical of Tarim and Middle Tienshan igneous rocks emplaced in a setting of rifting and/or active margin possibly related to the break-up of Rodinia (Zhu *et al*. 2011; Zhang *et al*. 2013). There are small outcrops of 650–600 Ma igneous rocks in northern Tarim, however no notable peaks of those ages in detrital zircon age patterns have been reported from Tarim (Zhu *et al*. 2011; Zhang *et al*. 2013; Rojas-Agramonte *et al*. 2014). On the contrary, the Kyzylkum-Nurata sandstones carry numerous detrital zircons with ages in the range of 650–570 Ma to form major peaks in their age patterns (Figures. 8, 14). Conclusively, the basement of the Karakum continent is probably similar in composition and age to the basement of the Tarim Craton, but may contain a larger proportion of Neoarchean rocks overprinted by younger Ediacaran – early Cambrian age events of tectonics and magmatism.

Another option for the deposition of both Ediacaran and Ordovician-Silurian sandstones carrying Precambrian zircons and having variable petrographic compositions and whole-rock Nd and Hf-in-zircon isotope characteristics (Figures 7, 12, 13, 15) is their derivation from a recycled orogen (Figure 7(c)), which could be an Andean-type active margin or from an Island arc rifted off such an active margin. A good example is the Japanese Islands or Japanese Arc, which formed by the rifting of the Cretaceous active margin of the Asian continent and resulted in the opening of the Sea of Japan and subduction initiation (Khanchuk *et al*. 1989; Isozaki *et al*. 1990, 2010). The Japanese Arc has a Precambrian basement, but remains a site of active subduction and its related magmatism. The clastic rocks (sandstones) from accretionary complexes of different ages carry zircons from both coeval arcs and Precambrian basement (Isozaki *et al*. 2010; Isozaki 2019; Pastor-Galan *et al*. 2021). A similar setting (Andean – syn-collisional arc) was proposed for the Gissar area in the Tajik Tienshan (Worthington *et al*. 2017). The Baimen (or Bukantau) Island arc could be also rifted off the active margin to form an arc similar to that of the Japanese Islands, i.e. with an older basement.

5.3. Depositional environments and igneous protoliths of Kyzylkum-Nurata sandstones

The U-Pb age data from both igneous and sedimentary rocks indicate that volcanic arcs existed at active margins of the Turkestan Ocean in late Ordovician – early Silurian time (Figures. 8, 13, 14).The semi-coeval deposition of two major groups of lithologically similar clastic sediments, Ediacaran and Silurian, over the South Tienshan-Karakum terrane and their similar detrital zircon age patterns suggest similar geodynamic environments once existed at subduction zones of the Paleo-Asian or Turkestan Ocean (Figure 16).

Whole-rock major and trace element data (Figures 9–11) from the Ediacaran and Silurian sandstones and their Nd isotope characteristics (εNd(t) = – 6.5 to – 16.2; Figure 12(a)) suggest that the sandstones are mature clastic sediments derived from evolved (Precambrian) continental crust with minor participation of juvenile material. Biske and co-authors (Biske *et al*. 2021) suggest that those clastic sediments were deposited in marginal seas of the Turkestan Ocean. Unlike the Kyzylkum Ordovician-Silurian sandstones, the similar Silurian sediments exposed in Tajikistan contain abundant Ordovician and Silurian zircons derived from coeval Island arcs (Biske *et al*. 2019, 2021). The relatively little amount of juvenile component in the sandstones (Figures. 12, 13, 15) can be explained by their deposition in a provenance mostly sourced by Karakum continent with a limited input from coeval Palaeozoic Island arcs (Figure 16).

Evidence for the dominantly recycled character of igneous rocks in the provenance of the sandstones comes also from the broad peaks at 1000–570 Ma, smaller peaks at 2700–2400 Ma and several 2200–1550 Ma single ages present at all U-Pb age patterns (Figure 8). All the samples show clear young peaks at 610–560 Ma. The U-Pb age spectra of the Silurian sandstones have the youngest narrow peak at ca. 445 Ma. These youngest detrital zircon grains may come from Ediacaran to Silurian Island arcs, probable sources of juvenile material.

5.4. Geodynamics implications and subduction erosion of Neoproterozoic and early Palaeozoic Island arcs

A dilemma exists between the major peaks at 870–730 and 650–570 Ma in the age patterns of all sandstones under consideration, which both contain zircons with juvenile Hf isotope characteristics (Figure. 12(b), 13). In northern Tarim and Middle Tienshan, the 870 to 730 Ma juvenile magmatic rocks are often linked with the break-up of Rodinia and/or Gondwana active margins (Zhu *et al*. 2011; Zhang *et al*. 2013; Rojas-Agramonte *et al*. 2014; Konopelko *et al*. 2017).

A relatively large amount of the 870–730 Ma detrital zircons from both Tarim and Kyzylkum have juvenile Hf characteristics (Figure 15). We suggest that the Tonian magmatism also affected the Karakum continent to deliver ca. 870–730 Ma detrital zircons (Figure 16).

In contrast to the Tonian zircons derived from the rocks related to the break-up of Rodinia, the sources of the Ediacaran detrital zircons and their origins remain debatable. The Cambrian active margin magmatism is widely manifested in Northern Tienshan (Wang *et al.* 2018; Alexeiev *et al.* 2019; Konopelko *et al.* 2021), Kunlun (Zuza and Yin 2017; Zhang, 2019), Central Kazakhstan (Rojas-Agramonte *et al.* 2014; Samygin and Kheraskova 2019; Degtyarev *et al.* 2020), western Junggar (Ren *et al.* 2014) and Central Iran (Faryad *et al.* 2016). The Cryogenian to Ediacaran magmatic rocks are less abundant: in northern Tarim (Ge *et al.* 2013), western Junggar (Yang *et al.* 2012) and Tienshan (Yang *et al.* 2005; Konopelko *et al.* 2014; Alexeiev *et al.* 2019).

Tectonic or subduction erosion in the CAOB was first suggested based on the discrepancy between geological and isotope data (Safonova 2014, 2017; Safonova *et al.* 2015). Later, evidence for subduction erosion during the late Palaeozoic came from the South and Middle Tienshan terranes, where it resulted in significant crustal loss and disappearance of several major early Palaeozoic Island arcs (Alexeiev *et al.* 2016). Our new data show that about 20% of the Ediacaran to Silurian zircons have juvenile Hf isotopic compositions with εHf(t) values ranging from 0 to +10 compared to less 650–570 Ma zircon grains with positive to negative εHf(t) (-5 to +3) from Tarim (Figure 15). The positive εHf(t) values in a part of the analysed sandstones suggest their derivation from Island arcs. The Ediacaran clastic (meta)sediments of both Uzbek South Tienshan (this paper) and Tajik South Tienshan (Biske *et al.* 2021) carry abundant 650–570 Ma detrital zircons (Figures. 8, 13). However, there are no prominent Island-arc igneous terranes in the region, except for small outcrops, like those in the Tamdy Mts. (Dolgopolova *et al.* 2017; Figure 2(a)). We suggest that the Ediacaran magmatic arcs, which sourced those zircons, were destroyed by surface and basal subduction erosion.

Subduction erosion can be responsible for the disappearance of crustal blocks through partial destruction of the overriding lithospheric plate due to collapse of the forearc and/or basal erosion above the subduction channel (Scholl *et al.* 1980; Scholl and von Huene, 2007). Destruction of major crustal terranes by subduction erosion was established in many Mesozoic and Cenozoic convergent margins and detrital zircons provide evidence for the previous existence of such terranes, which is a common feature for Pacific-type orogenic belts (Isozaki *et al.* 2010; Safonova *et al.* 2015; Safonova 2017). Evidence for subduction erosion of the Ediacaran and early Palaeozoic Island arcs comes from several accretionary complexes of the CAOB, South Tienshan, central and eastern Kazakhstan and northern Mongolia. The Pacific-type
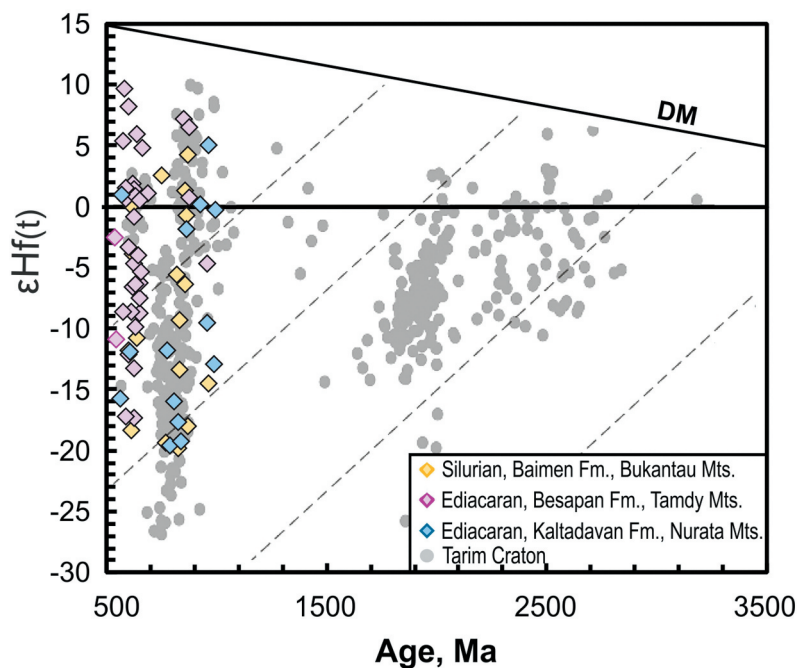
Figure 15. A summary of Hf-in-zircon isotope data from the Kyzylkum-Nurata sandstones (this study; He *et al.* 2014a, 2014b for Tarim).
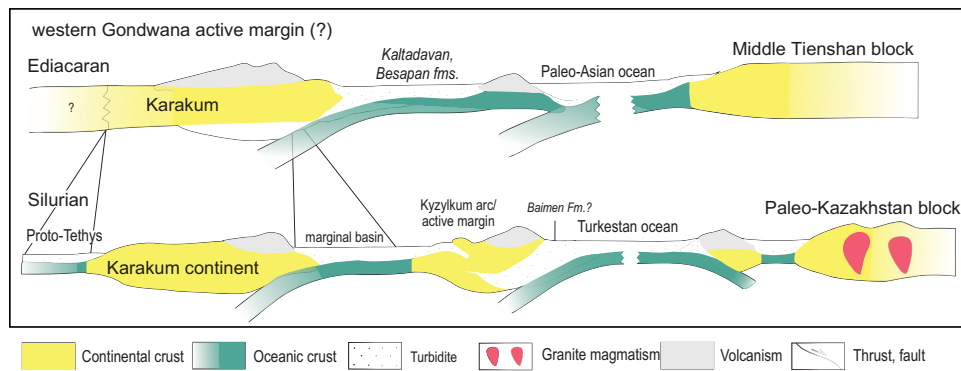
Figure 16. A cartoon showing geodynamics setting in the Paleo-Asian Ocean, including proto- Turkestan Ocean in Ediacaran-Silurian time (modified from Biske *et al.* 2021). In Ediacaran time, an active margin of Rodinia or Gondwana supplied to the subduction zone. The subduction of the Paleo-Asian Ocean formed intra-oceanic arc and accretionary complex hosting sedimentary and igneous rocks of ocean plate stratigraphy including accreted seamounts sediments (Taskazgan, Besapan and Kaltadavan fms.). Later, the Karakum continent rifted off Gondwana. In Silurian time, the subduction of the younger Turkestan Ocean under an active margin of the Karakum continent formed another volcanic arc and an accretionary complex (Baimen Fm.).

orogenic belts of those regions, host Ediacaran, Ordovician and Devonian arc-type igneous complexes occurring exotic tectonic blocks juxtaposed in tectonic mélanges with various Palaeozoic sediments, both oceanic plate stratigraphy, oceanic sediments and fore-arc clastic sediments (Safonova 2017; Alexeiev *et al.* 2020; Safonova *et al.* 2018, 2020, p. 2021; Savinskiy *et al.* in press). The presence of Ediacaran Island arc formations as tectonic blocks in the accretionary prism of the South Tienshan (Tamdy Mts.) coupled with the abundant Ediacaran detrital zircons in sediments of the whole western Tienshan indicate a major arc system, which existed at the southern active margin of the Turkestan ocean, possibly at the northern margin of the Karakum continent, in Ediacaran time. The subduction erosion of the Ediacaran arcs resulted in the termination of magmatism or magmatic lull in early Cambrian time (Figures. 8, 13). Later, the arc basements were uplifted/dissected to provide clastic material for the Palaeozoic sediments, which deposited at both landward and oceanward segments of the Karakum continent active margin (Figures. 8, 16).

The subduction erosion and its related cessation of magmatism in early Cambrian time resulted in the retreat of the subduction zone. The next important pulse of supra-subduction magmatism at the Karakum-South Tienshan active margin occurred in late Ordovician–early Silurian time. In the study area and in present-day coordinates, the Ediacaran subduction zone of the Tamdy area shifted to the north, i.e. to the Bukantau area, to initiate a new system of Island arcs at the southern active margin of the Turkestan Ocean (Biske *et al.* 2019). The late Ordovician–early Silurian active margin developed in shelf conditions in the Middle-late Devonian time to form thick Devonian-Carboniferous carbonate deposits

(Biske 1996, 2015). The late Devonian-Carboniferous shelf carbonate formation of the Turkestan Ocean can be traced from the Kyzylkum to the Chinese South Tienshan (Biske and Seltmann 2010). During the late Carboniferous collision, those carbonate platforms were thrust southward together with the obducted early Palaeozoic ophiolites, e.g. the 438 Ma ophiolite of the Tamdy Mts. (Dolgopolova *et al.* 2017). After the collision, during the early Permian, the whole region was intruded by post-collisional granitoids, which now occupy up to 30% of the territory of the Kyzylkum desert (Figure 2) (Konopelko *et al.* 2011; Dolgopolova *et al.* 2017; Konopelko 2020). Note that the early Permian post-collisional granitoids show significantly higher $\varepsilon Nd(t)$ (from −5 to +3) and $\varepsilon Hf(t)$ (from −5 to +12) values (Dolgopolova *et al.* 2017) than the Kyzylkum Ediacaran and Silurian clastic sedimentary rocks (Figures. 12, 13, 15). Such a discrepancy has been previously mentioned for the adjacent orogenic belts of Altai (Chen and Jahn 2002) and Pamir (Robinson *et al.* 2012). Therefore, the Kyzylkum clastic sediment unlikely served a major source for the post-collisional granitoids, but likely contaminated their parental granitoid melts (Chen and Jahn 2002).

The Silurian arcs were also probably destroyed by subduction erosion, but to a lesser extent compared to the Ediacaran arcs. Evidence for the Ordovician-Silurian arc magmatism is much better preserved in the accretionary complexes of the South and Middle Tienshan as they include numerous occurrences of Silurian ophiolites, granitoids and volcanic rocks of supra-subduction origin and their associated clastic rocks with lithic volcanic fragments (Dolgopolova *et al.* 2017; Biske *et al.* 2019; Alexeiev *et al.* 2020). According to the criteria highlighted in (Maruyama

et al. 2011; Safonova 2017; Safonova and Khanchuk 2021), among the three localities under consideration, i.e. Tamdy, Bukantau and Nuratau, at least the Tamdy (Besapan Fm.) and the Bukantau (Baimen Fm.) mountains obviously represent remnants of, respectively, Ediacaran and Ordovician-Silurian Pacific-type orogenic belts. Evidence for that comes from the presence of pieces of accreted ocean plate stratigraphy units with pelagic chert and oceanic pillow-lavas (Figures 3–5) and pieces of Island arc formations (Dalimov and Ganiev 2010; Dolgopolova *et al.* 2017). Moreover, the close location of supra-subduction igneous rocks and coeval turbidites in these two belts (Figures 2–5) suggest subduction erosion of older accreted units (Isozaki *et al.* 2010; Safonova *et al.* 2015; Safonova 2017). The U-Pb detrital zircon age pattern from the sandstones of the Baimen Fm. of the Bukantau Mts. is characterized by the small Silurian peak, but much larger Precambrian peaks (Figure 8(c)). In addition, the whole-rock Nd and Hf-in-zircon isotope data from those sandstones indicate that they were derived from ancient continental crust with minor contribution from juvenile sources (Figures. 12, 13). Therefore, the Silurian sandstones of the Baimen Fm. could have been deposited in internal parts of the continent where the input from coeval Palaeozoic Island arcs was limited or in a back-arc basin where clastic material was delivered from both the arc and the continental margin (Figure 16).

6. Conclusions

The deformed pre-Devonian clastic sediments occupy a major part of the vast Kyzylkum Desert in Uzbekistan and comprise a thick turbidite-type complex. We studied sandstones of the Besapan, Baimen and Kaltadavan formations outcropped in the Tamdytau, Bukantau and northern Nuratau mountain ranges, respectively. The Ediacaran Kaltadavan and Besapan formations consist of thick variably metamorphosed rhythmically bedded flyshoid-type sediments. The younger Silurian turbidites of the Baimen Fm. constitute several tectonic sheets. Most of the Kyzylkum-Nurata sandstones are spatially associated with oceanic plate stratigraphy rocks: pillowed basalt, pelagic chert, hemipelagic siliceous mudstone and siltstone, as well as with igneous rocks of supra-subduction origin.

All sandstone samples yielded similar U-Pb detrital zircon age patterns with major peaks at ca. 650–570, 870–730, 1050–900 and 2400 Ma and a smaller peak at 1800 Ma. These patterns are similar to the U-Pb zircon age spectra from the Tarim basement and the Tajik South Tienshan indicating similar depositional environments and sources. However, the Baimen samples from the Bukantau Mts. also show a peak at ca. 440 Ma. The maximum depositional ages of four sandstone samples of the Besapan and Kaltadavan formations vary in the range of 570–540 Ma. They indicate that a major part of pre-Devonian sediments deposited within a relatively narrow time interval of 50–70 Myrs from the latest Neoproterozoic (Ediacaran) to the earliest Cambrian. The Silurian Baimen Fm. sandstones yielded maximum depositional ages in the range from 500 to 400 Ma suggesting another, probably, less extended period of sedimentation.

Petrographic characteristics of the Ediacaran and Silurian sandstones are indicative of their generally grey-wacke and litharenite compositions and derivation from a recycled orogen, which could be either subduction complex or fold-and-thrust belt. The concentrations of major oxides in the sandstones are generally higher than those of PAAS, however, their trace element compositions resemble those of arc-related igneous rocks. The Nd isotope characteristics from sandstones (εNd(t) ranging from -16 to -9) suggest that the rocks represent mature sediments derived from igneous rocks containing recycled zircons with subordinate involvement of juvenile component. The presence of 650–570 Ma detrital zircons with juvenile Hf isotope characteristics in all samples suggests their derivation from igneous arcs. The dominantly greywacke composition of the sandstones, the trace element data and the Hf isotope characteristics are all indicative of two periods of subduction-related orogeny: latest Neoproterozoic – earliest Cambrian and Ordovician-Silurian. The U-Pb ages of detrital zircons from sandstones of the Kyzylkum-Nurata segments and adjacent regions show a middle-late Cambrian magmatic lull.

The new data from the Kyzylkum-Nurata sandstones and the presence of exotic tectonic blocks of Ediacaran arc-type rocks in the South Tienshan accretionary belt highlighted by previous researchers suggest an extended arc system once existed at the southern active margin of the Turkestan Ocean. That arc system could deliver clastic material for the Kyzylkum Palaeozoic sediments. The one or more arcs could be continental, i.e. Andean-type, or Japanese-type, i.e. intra-oceanic but built over ancient basement. The Ediacaran and Silurian sandstones probably deposited in the landward parts of, respectively, Ediacaran and Ordovician-Silurian Andean-type active margins of the Turkestan Ocean. The middle-late Cambrian magmatic lull and tectonic juxtaposition of arc-type magmatic rocks and coeval turbidite complexes in the Tamdy and Bukantau belts suggest early Palaeozoic subduction erosion.

Acknowledgments

Disclosure statement

No potential conflict of interest was reported by the author(s).

Funding

References

Akhmedov, N.A., 2000, Stratified and intrusive formations of Uzbekistan: Tashkent, 511 p. IMR Publishing House, in Russian

Akhmedov, N.A., Isakhodzhaev, B.A., and Abdusaimova, Z.M., 2001, Stratigraphic code of Uzbekistan: IMR Publishing House, Tashkent, 580 p. in Russian

Alexeiev, D.V., Biske, G.S., Kröner, A., Tretyakov, A.A., Kovach, V. P., and Rojas-Agramonte, Y., 2020, Ediacaran, Early Ordovician and early Silurian arcs in the South Tianshan orogen of Kyrgyzstan: Journal of Asian Earth Sciences, v. 190, 104194 p. doi:10.1016/j.jseaes.2019.104194.

Alexeiev, D.V., Kröner, A., Hegner, E., Rojas-Agramonte, Y., Biske, Y.S., Wong, J., Geng, H.Y., Ivleva, E.A., Mühlberg, M., Mikolaichuk, A.V., and Liu, D., 2016, Middle to Late Ordovician arc system in the Kyrgyz Middle Tianshan: From arc–continent collision to subsequent evolution of a Palaeozoic continental margin: Gondwana Research, v. 39, 261–291 p. doi:10.1016/j.gr.2016.02.003.

Alexeiev, D.V., Kröner, A., Kovach, V.P., Tretyakov, A.A., Rojas-Agramonte, Y., Degtyarev, K.E., Mikolaichuk, A.V., Wong, J., and Kiselev, V.V., 2019, Evolution of Cambrian and early Ordovician arcs in the Kyrgyz North Tianshan: Insights from U-Pb zircon ages and geochemical data: Gondwana Research, v. 66, 93–115 p. doi:10.1016/j.gr.2018.09.005.

Bhatia, M.R., and Crook, K.A.W., 1986, Trace element characteristics of greywacke and tectonic setting discrimination of sedimentary basins: Contributions to Mineralogy and Petrology, v. 92, no. 2, p. 181–193. doi:10.1007/BF00375292.

Biske, Y.S., 1996, Paleozoic structure and history of Southern Tian-Shan: St.-Petersburg University Publishing House, St. Petersburg, 190 p. In Russian

Biske, Y.S., Alexeiev, D.V., Ershova, V.B., Priyatkina, N.S., DuFrane, S.A., and Khudoley, A.K., 2019, Detrital zircon U-Pb geochronology of middle Paleozoic sandstones from the South Tianshan (Kyrgyzstan): Implications for provenance and tectonic evolution of the Turkestan Ocean: Gondwana Research, v. 75, 97–117 p. doi:10.1016/j.gr.2019.04.010.

Biske, Y.S., Ershova, V.B., Konopelko, D.L., Stockli, D., Mamadjanov, Y.M., and Wang, X.S., 2021, Detrital-zircon geochronology and provenance of Ediacaran–Silurian rocks of the central to northern Tajikistan traverse: Geodynamic implications for the evolution of the Tian Shan: Gondwana Research, v. 99, 247–268 p. doi:10.1016/j.gr.2021.07.013.

Biske, Y.S., 2015, Geology and evolution of the Central Asian Orogenic Belt in Kazakhstan and the western Tianshan, in Kroner, A., ed., The Central Asian orogenic Belt. Geology, evolution, tectonics and models: Stuttgart, Borntraeger Science Publishers, p. 6–49.

Biske, Y.S., and Seltmann, R., 2010, Paleozoic Tian-Shan as a transitional region between the Rheic and Urals–Turkestan oceans: Gondwana Research, v. 17, no. 2–3, p. 602–613. doi:10.1016/j.gr.2009.11.014.

Black, L.P., and Jagodzinski, E.A., 2003, Importance of establishing sources of uncertainty for the derivation of reliable SHRIMP ages: Australian Journal of Earth Sciences, v. 50, no. 4, p. 503–512. doi:10.1046/j.1440-0952.2003.01007.x.

Black, L.P., Kamo, S.L., Allen, C.M., Aleinikoff, J.N., Davis, D.W., Korsch, R.J., and Foudoulis, C., 2003, TEMORA 1: A new zircon standard for U-Pb geochronology: Chemical Geology, v. 200, no. 1–2, p. 155–170. doi:10.1016/S0009-2541(03)00165-7.

Bukharin, A.K., Maslennikova, I.A., and Piatkov, A.K., 1985, Pre-Mezozoic structure-facial zones of the Western Tian-Shan: Fan, Tashkent, 152 p. in Russian

Burtman, V.S., 1975, Structural geology of Variscan Tien Shan, USSR: American Journal of Science, v. 275-A, p. 157–186.

Burtman, V.S., 2015, Tectonics and geodynamics of the Tian Shan in the middle and late Paleozoic: Geotectonics, v. 49, no. 4, p. 302–319. doi:10.1134/S0016852115040020.

Chen, B., and Jahn, B.-M., 2002, Geochemical and isotopic studies of the sedimentary and granitic rocks of the Altai orogen of northwest China and their tectonic implications: Geological Magazine, v. 139, no. 1, p. 1–13. doi:10.1017/S0016756801006100.

Chiaradia, M., Konopelko, D., Seltmann, R., and Cliff, R.A., 2006, Lead isotope variations across terrane boundaries of the Tienshan and Chinese Altay: Mineralium Deposita, v. 41, no. 5, p. 411–428. doi:10.1007/s00126-006-0070-x.

Condie, K.C., 1993, Chemical composition and evolution of the upper continental crust – Contrasting results from surface samples and shales: Chemical Geology, v. 104, no. 1–4, p. 1–37. doi:10.1016/0009-2541(93)90140-E.

Cox, R., Lowe, D.R., and Cullers, R., 1995, The influence of sediment recycling and basement composition on evolution of mudrock chemistry in the southwestern United States: Geochimica et Cosmochimica Acta, v. 59, no. 14, p. 2919–2940. doi:10.1016/0016-7037(95)00185-9.

Cullers, R.L., and Podkovyrov, V.N., 2000, Geochemistry of the Mesoproterozoic Lakhanda shales in southeastern Yakutia, Russia: Implications for mineralogical and provenancecontrol, and recycling: Precambrian Research, v. 104, no. 1–2, p. 77–93. doi:10.1016/S0301-9268(00)00090-5.

Dalimov, T.N., and Ganiev, I.N., 2010, Evolution and type of magmatism in the western Tian-Shan: Tashkent, 226 p. IMR Publishing House, in Russian

Degtyarev, K.E., Yakubchuk, A.S., Luchitskaya, M.V., and Tretyakov, A.A., 2020, Age and structure of a fragment of the Early Cambrian ophiolite sequence (north Balkhash zone, central Kazakhstan): Doklady Earth Sciences, v. 491, no. 1, p. 111–116. doi:10.1134/S1028334X20030034.

Dickinson, W.R., Berad, L.S., Brakenridge, G.R., Erjavec, J.L., Ferguson, R.C., Inman, K.F., Knepp, R.A., Lindberg, F.A., and Ryberg, P.T., 1983, Provenance of North American Phanerozoic sandstones in relation-to-tectonic-setting: GSA Bulletin, v. 94, no. 2, p. 222–235. doi:10.1130/0016-7606(1983)94<222:PONAPS>2.0.CO;2.

Dolgopolova, A., Seltmann, R., Konopelko, D., Biske, Y.S., Shatov, V., Armstrong, R., Belousova, E., Pankhurst, R., Koneev, R., and Divaev, F., 2017, Geodynamic evolution of the western Tienshan, Uzbekistan: Insights from U-Pb SHRIMP geochronology and Sr-Nd-Pb-Hf isotope mapping of granitoids: Gondwana Research, v. 47, 76–109 p. doi:10.1016/j.gr.2016.10.022.

Faryad, S.W., Collett, S., Finger, F., Sergeev, S.A., Čopjaková, R., and Siman, P., 2016, The Kabul Block (Afghanistan), a segment of the Columbia Supercontinent, with a Neoproterozoic metamorphic overprint: Gondwana Research, v. 34, 221–240 p. doi:10.1016/j.gr.2015.02.019.

Floyd, P.A., and Leveridge, B.E., 1987, Tectonic environment of the Devonian Gramscatho basin, south Cornwall: Framework mode and geochemical evidence from turbiditic sandstones: Journal of the Geological Society, v. 144, no. 4, p. 531–542. doi:10.1144/gsjgs.144.4.0531.

Folk, R.L., 1980, Petrology of sedimentary rocks: Hemphill. Austin, Texas, 182 p.

Ge, R., Zhu, W., Wu, H., Zheng, B., and He, J., 2013, Timing and mechanisms of multiple episodes of migmatization in the Korla Complex; northern Tarim Craton; NW China: Constraints from zircon U–Pb–Lu–Hf isotopes and implications for crustal growth: Precambrian Research, v. 231, 136–156 p. doi:10.1016/j.precamres.2013.03.005.

Ghes, M.D., 2008, Terrane structure and geodynamic evolution of the caledonides of Tian-Shan: Altyn Tamga Publishing House, Bishkek, 158 p. in Russian

Glorie, S., Jepson, G., Konopelko, D., Mirkamalov, R., Meeuws, F., Gilbert, S., Gillespie, J., Collins, A.S., Xiao, W.J., Dewaele, S., and De Grave, J., 2019, Thermochronological and geochemical footprints of post-orogenic fluid alteration recorded in apatite: Implications for mineralisation in the Uzbek Tian Shan: Gondwana Research, v. 71, p. 1–15. doi:10.1016/j.gr.2019.01.011.

Han, Y.G., Zhao, G.C., Sun, M., Eizenhöfer, P.R., Hou, W.Z., Zhang, X.R., Liu, D.X., Wang, B., and Zhang, G.W., 2015, Paleozoic accretionary orogenesis in the Paleo- Asian Ocean: Insights from detrital zircons from Silurian to Carboniferous strata at the northwestern margin of the Tarim Craton: Tectonics, v. 34, no. 2, p. 334–351. doi:10.1002/2014TC003668.

He, J.W., Zhu, W.B., Ge, R.F., Zheng, B.H., and Wu, H.L., 2014b, Detrital zircon U-Pb ages and Hf isotopes of Neoproterozoic strata in the Aksu area, northwestern Tarim Craton: Implications for supercontinent reconstruction and crustal evolution: Precambrian Research, v. 254, p. 194–209. doi:10.1016/j.precamres.2014.08.016.

He, J., Zhu, W., and Ge, R., 2014a, New age constraints on Neoproterozoic diamicites in Kuruktag, NW China and Precambrian crustal evolution of the Tarim Craton: Precambrian Research, v. 241, p.44–60 doi:10.1016/j.precamres.2013.11.005.

Isozaki, Y., 2019, A visage of early Paleozoic Japan: Geotectonic and paleobiogeographical significance of Greater South China: Island Arc, v. 28, no. 3, e12296 p. doi:10.1111/iar.12296.

Isozaki, Y., Aoki, K., Nakama, T., and Yanai, S., 2010, New insight into a subduction-related orogen: A reappraisal of the geotectonic framework and evolution of the Japanese Islands: Gondwana Research, v. 18, no. 1, p. 82–105. doi:10.1016/j.gr.2010.02.015.

Isozaki, Y., Maruyama, S., and Fukuoka, F., 1990, Accreted oceanic materials in Japan: Tectonophysics, v. 181, no. 1–4, p. 179–205. doi:10.1016/0040-1951(90)90016-2.

Kanygina, N.A., Tretyakov, A.A., Degtyarev, K.E., Kovach, V.P., Skuzovatov, S.Y., Pang, K.N., Wang, K.L., and Lee, H.Y., 2021, Late Mesoproterozoic–early Neoproterozoic quartzite–schist sequences of the Aktau–Mointy terrane (Central Kazakhstan): Provenance, crustal evolution, and implications for paleotectonic reconstruction: Precambrian Research, v. 354, 106040 p. doi:10.1016/j.precamres.2020.106040.

Käßner, A., Ratschbacher, L., Pfänder, J.A., Hacker, B.R., Sonntag, B., Stanek, K.P., Stanek, K.P., Zack, G., Gadoev, M., and Oimahmadov, I., 2017, Proterozoic-Mesozoic history of the Central Asian orogenic belt in the Tajik and southwestern Kyrgyz Tian Shan: UPb, ${}^{40}Ar/{}^{39}Ar$, and fission-track geochronology and geochemistry of granitoids: Geological Society of America Bulletin, v. 129, no. 3–4, p. 281–303. doi:10.1130/B31466.1.

Khanchuk, A.I., Kemkin, I.V., and Panchenko, I.V., 1989, Geodynamic evolution of sikhotealin and sakhalin in middle paleozoic and early mesozoic, in Scheglov, A.D., ed., Pacific Margin of Asia: Geology: Nauka, Moscow, p. 218–255. in Russian

Konopelko, D., 2020, Paleozoic granitoid magmatism of western Tien Shan. Saint Petersburg: Saint Petersburg University Publishing house, 196 p. in Russian. doi:10.21638/11701/9785288060250.

Konopelko, D., Biske, G., Kullerud, K., Seltmann, R., and Divaev, F., 2011, The Koshrabad granite massif in Uzbekistan: Petrogenesis, metallogeny and geodynamic setting: Russian Geology and Geophysics, v. 52, no. 12, p. 1563–1573. doi:10.1016/j.rgg.2011.11.009.

Konopelko, D., Biske, G., Seltmann, R., Petrov, S.V., and Lepekhina, E., 2014, Age and petrogenesis of the Neoproterozoic Chon-Ashu alkaline complex, and a new discovery of chalcopyrite mineralization in the eastern Kyrgyz Tienshan: Ore Geology Reviews, v. 61, 175–191 p. doi:10.1016/j.oregeorev.2014.02.004.

Konopelko, D., Biske, Y.S., Kullerud, K., Ganiev, I., Seltmann, R., Brownscombe, W., Mirkamalov, R., Wang, B., Safonova, I., Kotler, P., Shatov, V., Sun, M., and Wong, J., 2019, Early Carboniferous metamorphism of the Neoproterozoic South

Tienshan-Karakum basement: New geochronological results from Baisun and Kyzylkum, Uzbekistan: Journal of Asian Earth Sciences, v. 177, 275–286 p. doi:10.1016/j.jseaes.2019.03.025.

Konopelko, D., and Klemd, R., 2016, Deciphering protoliths of the (U)HP rocks in the Makbal metamorphic complex, Kyrgyzstan: Geochemistry and SHRIMP zircon geochronology: European Journal of Mineralogy, v. 28, no. 6, p. 1233–1253. doi:10.1127/ejm/2016/0028-2602.

Konopelko, D., Klemd, R., Mamadjanov, Y., Hegner, E., Knorsch, M., Fidaev, D., Kern, M., and Sergeev, S., 2015, Permian age of orogenic thickening and crustal melting in the Garm Block, South Tienshan, Tajikistan: Journal of Asian Earth Sciences, v. 113, 711–727 p. doi:10.1016/j.jseaes.2015.09.004.

Konopelko, D., Klemd, R., Petrov, S.V., Apayarov, F., Nazaraliev, B., Vokueva, O., Schersten, A., and Sergeev, S., 2017, Precambrian gold mineralization at Djamgyr in the Kyrgyz Tienshan: Tectonic and metallogenic implications: Ore Geology Reviews, v. 86, 537–547 p. doi:10.1016/j.oregeorev.2017.03.007.

Konopelko, D., Seltmann, R., Dolgopolova, A., Safonova, I., Glorie, S., De Grave, J., and Sun, M., 2021, Adakite-like granitoids of Songkultau: A relic of juvenile Cambrian arc in Kyrgyz Tienshan: Geoscience Frontiers, v. 12, no. 1, p. 147–160. doi:10.1016/j.gsf.2020.08.006.

Kröner, A., Kovach, V., Belousova, E., Hegner, E., Armstrong, R., Dolgopolova, A., Seltmann, R., Alexeiev, D.V., Hoffmann, J.E., Wong, J., Sun, M., Cai, K., Wang, T., Tong, Y., Wilde, S.A., Degtyarev, K.E., and Rytsk, E., 2014, Reassessment of continental growth during the accretionary history of the Central Asian orogenic belt: Gondwana Research, v. 25, p. 103–125.

Lomize, M.G., Demina, L.I., and Zarshchikov, A.A., 1997, The Kyrgyz-Terskei Paleo-oceanic Basin, Tienshan: Geodynamics Series, v. 6, p. 35–55.

Maruyama, S., Omori, S., Sensu, H., Kawai, K., and Windley, B.F., 2011, Pacific-type Orogens: New concepts and Variations in Space and Time from Present to Past: Journal of Geography, v. 120, no. 1, p. 115–223. in Japanese with English abstract and captions doi:10.5026/jgeography.120.115.

Maruyama, S., and Safonova, I.Y., 2019, Orogeny and mantle dynamics: Role of tectonic erosion and second continent in the mantle transition zone: IPC NSU, 208 p.

McLennan, S.M., 1989, Rare earth elements in sedimentary rocks: Influence of provenance and sedimentary processes, in Lipin, B.R., and McKay, G.A., eds., Geochemistry and Mineralogy of Rare Earth Elements: p. 169–200. Mineralogical Society of America, Washington, D.C.,

Mirkamalov, R.H., Chirikin, V.V., Khan, R.S., Kharin, V.G., and Sergeev, S.A., 2012, Results of U-Pb (SHRIMP) dating of granitoid and metamorphic complexes of the Tienshan fold belt (Uzbekistan): Vestnik SPbGU, v. 7, no. 1, p. 3–25. in Russian

Mukhin, P.A., Karimov, K.K., and Savchuk, Y.S., 1991, Paleozoic geodynamics of the Kyzylkum: FAN, Tashkent, 148 p. in Russian

Mukhin, P.A., Savchuk, Y.S., and Kolesnikov, A.V., 1988, Position of the "Muruntau lens" within the collage of metamorphic units in the Southern Tamdytau (Central Kyzylkum desert): Geotectonics, v. 22, no. 2, p. 142–148.

Nance, W., and Taylor, S., 1976, Rare earth element patterns and crustal evolution. Australian post-Archean sedimentary rocks: Geochimica et Cosmochimica Acta, v. 40, no. 12, p. 1539–1551. doi:10.1016/0016-7037(76)90093-4.

Nesbitt, H.W., and Young, G.M., 1982, Early Proterozoic climates and plate motions inferred from major element chemistry of lutites: Nature, v. 299, no. 5885, p. 715–717. doi:10.1038/299715a0.

Nesbitt, H., and Young, G., 1984, Prediction of some weathering trends of plutonic and volcanic rocks based on thermodynamic and kinetic considerations: Geochimica et Cosmochimica Acta, v. 48, no. 7, p. 1523–1534. doi:10.1016/0016-7037(84)90408-3.

Pastor-Galan, D., Spencer, C.J., Furukawa, T., and Tsujimori, T., 2021, Evidence for crustal removal, tectonic erosion and flare-ups from the Japanese evolving forearc sediment provenance: Earth and Planetary Science Letters, v. 564, 116893 p. doi:10.1016/j.epsl.2021.116893.

Pettijohn, F.J., Potter, P.E., and Siever, R., 1972, Sand and Sandstones: New York, Springer-Verlag, 618 p.

Ren, R., Han, B.F., Xu, Z., Zhou, Y.Z., Liu, B., Zhang, L., Liu, B., Zhang, L., Chen, J.-F., Su, L., Li, J., Li, Z.-H., and Li, Q.-L., 2014, When did the subduction first initiate in the southern Paleo-Asian Ocean: new constrains from a cambrian intra-oceanic arc system in West Junggar, NW China: Earth and Planetary Science Letters, v. 388, 222–236 p. doi:10.1016/j.epsl.2013.11.055.

Robinson, A.C., Ducea, M., and Lapen, T.J., 2012, Detrital zircon and isotopic constraints on the crustal architecture and tectonic evolution of the northeastern Pamir: Tectonics, v. 31, no. 2, doi:10.1029/2011TC003013.

Rojas-Agramonte, Y., Kröner, A., Alexeiev, D.V., Jeffreys, T., Khudoley, A.K., Wong, J., Geng, H., Shug, L., Semiletkin, S.A., Mikolaichuk, A.V., Kiselev, V.V., Yangj, J., and Seltmann, R., 2014, Detrital and igneous zircon ages for supracrustal rocks of the Kyrgyz Tianshan and palaeogeographic implications: Gondwana Research, v. 26, no. 3–4, p. 957–974. doi:10.1016/j.gr.2013.09.005.

Safonova, I., 2017, Juvenile versus recycled crust in the central asian orogenic belt: implications from ocean plate stratigraphy, blueschist belts and intra-oceanic arcs: Gondwana Research, v. 47, 6–27 p. doi:10.1016/j.gr.2016.09.003.

Safonova, I., Biske, G., Romer, R.L., Seltmann, R., Simonov, V., and Maruyama, S., 2016, Middle paleozoic mafic magmatism and ocean plate stratigraphy of the South Tianshan, Kyrgyzstan: Gondwana Research, v. 30, 236–256 p. doi:10.1016/j.gr.2015.03.006.

Safonova, I., Maruyama, S., Kruk, N., Obut, O., Kotler, P., Gavryushkina, O., Khromykh, S., Kuibida, M., and Krivonogov, S., 2018, Pacific-type orogenic belts: Linking evolution of oceans, active margins and mantle magmatism: Episodes, v. 41, no. 2, p. 79–88. doi:10.18814/epiiugs/2018/018008.

Safonova, I., Maruyama, S., and Litasov, K., 2015, Generation of hydrous-carbonated plumes in the mantle transition zone linked to tectonic erosion and subduction: Tectonophysics, v. 662, 454–471 p. doi:10.1016/j.tecto.2015.08.005.

Safonova, I., Perfilova, A., Obut, O., Kotler, P., Aoki, S., Komiya, T., Wang, B. & Sun, M., 2021. Traces of intra-oceanic arcs recorded in sandstones of eastern Kazakhstan: implications from U–Pb detrital zircon ages, geochemistry, and Nd–Hf isotopes. Int J Earth Sci (Geol Rundsch) (2021). doi:10.1007/s00531-021-02059-z

Safonova, I., 2014, Evaluation of juvenile versus recycled crust in the central asian orogenic belt: Importance of OPS, HP belts and fossil arcs, in Santosh, M., Pradeepkumar, A.P., and Shaji, E., eds., The 2014 Convention and 11th International Conference on "Gondwana to Asia", abstract volume, China University of Geosciences, Beijing, September 20–21. International Association for Gondwana Research Conference Series 20, p. 115–117.

Safonova, I., Savinskiy, I., Perfilova, A., Gurova, A., and Maruyama, S., 2020, The Itmurundy Pacific-type orogenic belt in northern Balkhash, central Kazakhstan: Revisited plus first U-Pb age, geochemical and Nd isotope data from igneous rocks: Gondwana Research, v. 79, 49–69 p. doi:10.1016/j.gr.2019.09.004.

Safonova, I., Seltmann, R., Kröner, A., Gladkochub, D., Schulmann, K., Xiao, W., Kim, T., Komiya, T., and Sun, M., 2011, A new concept of continental construction in the Central Asian Orogenic Belt (compared to actualistic examples from the Western Pacific): Episodes, v. 34, no. 3, p. 186–194. doi:10.18814/epiiugs/2011/v34i3/005.

Safonova, I.Y., and Khanchuk, A.I., 2021, Subduction erosion at Pacific-type convergent margins: Russian Journal of Pacific Geology, v. 40, no. 6, p. 3–19.

Samygin, S.G., and Kheraskova, T.N., 2019, Geology and tectonic evolution of Kazakhstan Paleozoides: Litosfera, v. 19, no. 3, p. 347–371. in Russian

Savchuk, Y.S., Asadulin, E.E., Volkov, A.V., and Aristov, V., 2018, The muruntau deposit: geodynamic position and a variant of genetic model of the Ore-Forming system: Geology of Ore Deposits, v. 60, no. 5, p. 365–397. doi:10.1134/S1075701518050069.

Savchuk, Y.S., Mukhin, P.A., and Meshcheryakova, L.V., 1991, Late Paleozoic granitoid magmatism and Kyzylkum ore formations from a plate tectonics point of view: Geotectonics, v. 25, no. 4, p. 326–339.

Savinskiy, I., Safonova, I., Perfilova, A., Kotler, P., Sato, T., and Maruyama, S., in press, A story of Devonian ocean plate stratigraphy hosted by the Ulaanbaatar accretionary complex, northern Mongolia: Implications from geological, structural and U-Pb detrital zircon data: International Journal of Earth Sciences,

Scholl, D.W., and van Huene, R., 2007, Crustal recycling at modern subduction zones applied to the past - Issues of growth and preservation of continental basement crust, mantle geochemistry, and supercontinent reconstruction: Geological Society of America Memoirs, v. 200, p. 9–32.

Scholl, D.W., Von Huene, R., Vallier, T.L., and Howell, D.G., 1980, Sedimentary masses and concepts about tectonic processes at underthrust ocean margins: Geology, v. 8, no. 12, p. 564–568. doi:10.1130/0091-7613(1980)8<564:SMACAT>2.0.CO;2.

Seltmann, R., Goldfarb, R.J., Zu, B., Creaser, R.A., Dolgopolova, A., and Shatov, V.V., 2020, Muruntau, Uzbekistan: The World's Largest Epigenetic Gold Deposit: SEG Special Publications, v. 23, p. 497–521.

Seltmann, R., Konopelko, D., Biske, G., Divaev, F., and Sergeev, S., 2011, Hercynian postcollisional magmatism in the context of Paleozoic magmatic evolution of the Tienshan orogenic belt: Journal of Asian Earth Sciences, v. 42, no. 5, p. 821–838. doi:10.1016/j.jseaes.2010.08.016.

Shutov, V.D., 1967, Classification of sandstones: Litologiya I Poleznyie Iskopaemyie, v. 5, p. 86–102. in Russian

Sun, S.S., and McDonough, W.F., 1989, Chemical and isotopic systematic of oceanic basalts; implications for mantle composition and processes, in Saunders, A.D., and Norry, M.J., eds., Magmatism in the Ocean Basins: Geological Society of London, Special Publication, Vol. 42, p. 313–345.

Taylor, S.R., and McLennan, S.H., 1985, The Continental Crust: Its Composition and Evolution. Blackwell: Oxford, 312 p.

Wang, X.-S., Klemd, R., Gao, J., Jiang, T., Li, J.-L., and Xue, S.-C., 2018, Final assembly of the southwestern Central Asian Orogenic Belt as constrained by the evolution of the South Tianshan Orogen: Links with Gondwana and Pangea. Journal of Geophysical Research: Solid Earth, v. 123, p. 7361–7388. doi:10.1029/2018JB015689

Windley, B.F., Alexeiev, D., Xiao, W., Kröner, A., and Badarch, G., 2007, Tectonic models for accretion of the Central Asian Orogenic Belt: Journal of the Geological Society of London, v. 164, no. 1, p. 31–47. doi:10.1144/0016-76492006-022.

Worthington, J.R., Kapp, P., Minaev, V., Chapman, J.B., Mazdab, F.K., Ducea, M.N., Oimahmadov, I., and Gadoev, M., 2017, Birth, life, and demise of the Andean – Syn-collisional Gissar arc: Late Paleozoic tectono-magmatic-metamorphic evolution of the southwestern Tian Shan, Tajikistan: Tectonics, v. 36, no. 10, p. 1861–1912. doi:10.1002/2016TC004285.

Xiao, W.J., Windley, B.F., Allen, M., and Han, C.M., 2013, Paleozoic multiple accretionary and collisional tectonics of the Chinese Tianshan orogenic collage: Gondwana Research, v. 23, p. 1316–1341.

Yang, G.X., Li, Y.J., Yang, B.K., Wang, H.B., Zhang, H.W., and Tong, L.L., 2012, Geochemistry of basalt from the Barleik ophiolitic mélange in West Junggar and its tectonic implications: Acta Geologica Sinica, v. 86, p. 188–197. in Chinese with English abstract

Yang, H.B., Gao, P., Li, B., and Zhang, Q.J., 2005, The geological character of the Sinian Dalubayi ophiolite in the west Tianshan, Xinjiang: Geology, v. 23, p. 123–126. in Chinese with English abstract

Zhang, C.-L., Zou, H.-B., Li, H.-K., and Wang, H.-Y., 2013, Tectonic framework and evolution of the Tarim Block in NW China: Gondwana Research, v. 23, no. 4, p. 1306–1315. doi:10.1016/j.gr.2012.05.009.

Zhang, C.-L., Zou, H.-B., Ye, X.-T., and Chen, X.-Y., 2019, Tectonic evolution of the West Kunlun Orogenic Belt along the northern margin of the Tibetan Plateau: Implications for the Assembly of the Tarim Terrane to Gondwana. Geoscience Frontiers, v. 10, p. 973–988.

Zhao, Z.H., Wang, Z.G., Zou, T.R., and Masuda, A., 1993, The REE, isotopic composition of O, Pb, Sr and Nd and petrogenesis of granitoids in the Altai region, in Tu, G.Z., ed., Progress of solid-earth sciences in northern Xinjiang: China:Beijing, Science Press, p. 239–266. in Chinese with English abstract

Zhu, W.B., Zheng, B.H., Shu, L.S., Ma, D.S., Wan, J.L., Zheng, D.W., Zhang, Z.Y., and Zhu, X.Q., 2011, Geochemistry and SHRIMP U–Pb zircon geochronology of the Korla mafic dykes: Constrains on the Neoproterozoic continental breakup in the Tarim Block, northwest China: Journal of Asian Earth Sciences, v. 42, no. 5, p. 791–804. doi:10.1016/j.jseaes.2010.11.018.

Zonenshain, L.P., Kuzmin, M.I., and Natapov, L.M., 1990, Geology of the USSR: A Platetectonic Synthesis. AGU Geodynamics Series 21: American Geophysical Union, Washington, DC, 242 p.

Zuza, A.V., and Yin, A., 2017, Balkatach hypothesis: A new model for the evolution of the Pacific, Tethyan, and Paleo-Asian oceanic domains: Geosphere, v. 13, no. 5, p. 1–49.